

A 3D cutaway diagram of the Mu2e experiment detector. The detector is a long, cylindrical structure composed of several sections. From left to right, it includes a series of green cylindrical modules, a central section with purple and blue components, and a final section with green cylindrical modules. A green wavy line representing a particle path is shown entering from the left and passing through the detector. The entire structure is mounted on a dark base.

# Mu2e : An Experimental Search for $\mu^- N \rightarrow e^- N$

Presented by Sophie Charlotte Middleton

Seminar at the University of Edinburgh

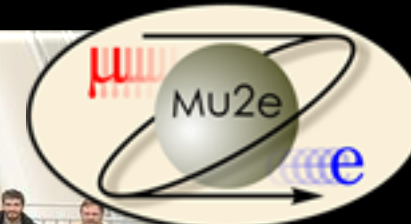
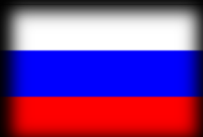
January 2021

[smidd@caltech.edu](mailto:smidd@caltech.edu)

# The Mu2e Collaboration



Argonne National Laboratory • Boston University Brookhaven National Laboratory Lawrence Berkeley National Laboratory and University of California, Berkeley • University of California, Davis • University of California, Irvine • California Institute of Technology • City University of New York • Joint Institute for Nuclear Research, Dubna • Duke University • Fermi National Accelerator Laboratory • Laboratori Nazionali di Frascati • INFN Genova • HelmholtzZentrum Dresden- Rossendorf • University of Houston • Institute for High Energy Physics, Protvino • Kansas State University • INFN Lecce and Università del Salento • Lewis University • University of Liverpool • University College London • University of Louisville • University of Manchester • Laboratori Nazionali di Frascati and Università Marconi Roma • University of Minnesota • Institute for Nuclear Research, Moscow • Muons Inc. • Northern Illinois University • Northwestern University • Novosibirsk State University/Budker Institute of Nuclear Physics • INFN Pisa • Purdue University • University of South Alabama • Sun Yat Sen University • University of Virginia • University of Washington • Yale University

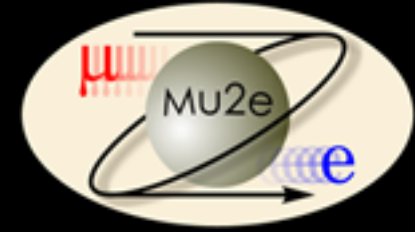


**Technical Design  
Report:**  
**arXiv: 1501.05241**



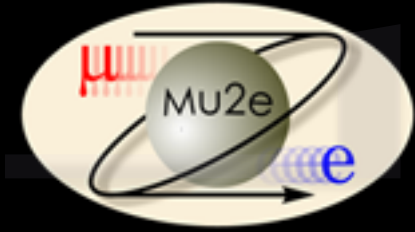
# Mu2e : An Experimental Search for $\mu^- N \rightarrow e^- N$

---



1. Flavor violation in Quarks and Neutral Leptons
2. Introducing Charged Lepton Flavor Violation (CLFV)
3. History: from muon discovery to current upper limits
4. The Global Search for CLFV and complementarity: Mu2e, MEG-II & Mu3e
5. CLFV & beyond Standard Model theories, how can we help?
6. The Mu2e Experiment:
  1. Limiting Standard Model Backgrounds
  2. Design
  3. Status
7. Summary

# The Standard Model

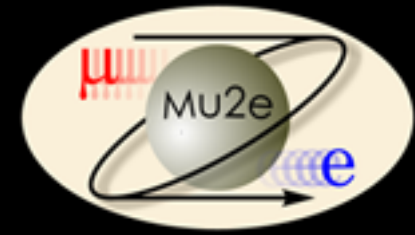


Quarks combine to form hadrons such as protons or neutrons.

Neutrinos were long believed massless but discovery of oscillations suggest they have small mass.

|         | 1 <sup>st</sup> Gen.  | 2 <sup>nd</sup> Gen.  | 3 <sup>rd</sup> Gen.   |  |
|---------|---|---|--|--|
| quarks  | $m = 2.3 \text{ MeV}$<br>$c = 2/3$<br>$s = 1/2$<br><b>u</b>               | $m = 1.28 \text{ GeV}$<br>$c = 2/3$<br>$s = 1/2$<br><b>c</b>                  | $m = 173.2 \text{ GeV}$<br>$c = 2/3$<br>$s = 1/2$<br><b>t</b>                  | $m = 0$<br>$c = 0$<br>$s = 1$<br><b><math>\gamma</math></b>  |
|         | $m = 4.8 \text{ MeV}$<br>$c = -1/3$<br>$s = 1/2$<br><b>d</b>              | $m = 95 \text{ MeV}$<br>$c = -1/3$<br>$s = 1/2$<br><b>s</b>                   | $m = 4.18 \text{ GeV}$<br>$c = -1/3$<br>$s = 1/2$<br><b>b</b>                  | $m = 0$<br>$c = 0$<br>$s = 1$<br><b><math>g</math></b>       |
|         | $m < 2.2 \text{ eV}$<br>$c = 0$<br>$s = 1/2$<br><b><math>\nu_e</math></b> | $m < 0.17 \text{ MeV}$<br>$c = 0$<br>$s = 1/2$<br><b><math>\nu_\mu</math></b> | $m < 15.5 \text{ MeV}$<br>$c = 0$<br>$s = 1/2$<br><b><math>\nu_\tau</math></b> | $m = 91.2 \text{ GeV}$<br>$c = 0$<br>$s = 1$<br><b>Z</b>     |
| leptons | $m = 0.511 \text{ MeV}$<br>$c = -1$<br>$s = 1/2$<br><b>e</b>              | $m = 105.7 \text{ MeV}$<br>$c = -1$<br>$s = 1/2$<br><b><math>\mu</math></b>   | $m = 1.777 \text{ GeV}$<br>$c = -1$<br>$s = 1/2$<br><b><math>\tau</math></b>   | $m = 80.4 \text{ GeV}$<br>$c = \pm 1$<br>$s = 1$<br><b>W</b> |
|         |   |   |  | $m = 125.18 \text{ GeV}$<br>$c = 0$<br>$s = 0$<br><b>H</b>   |
|         |   |   |  | <b>Higgs</b>   |

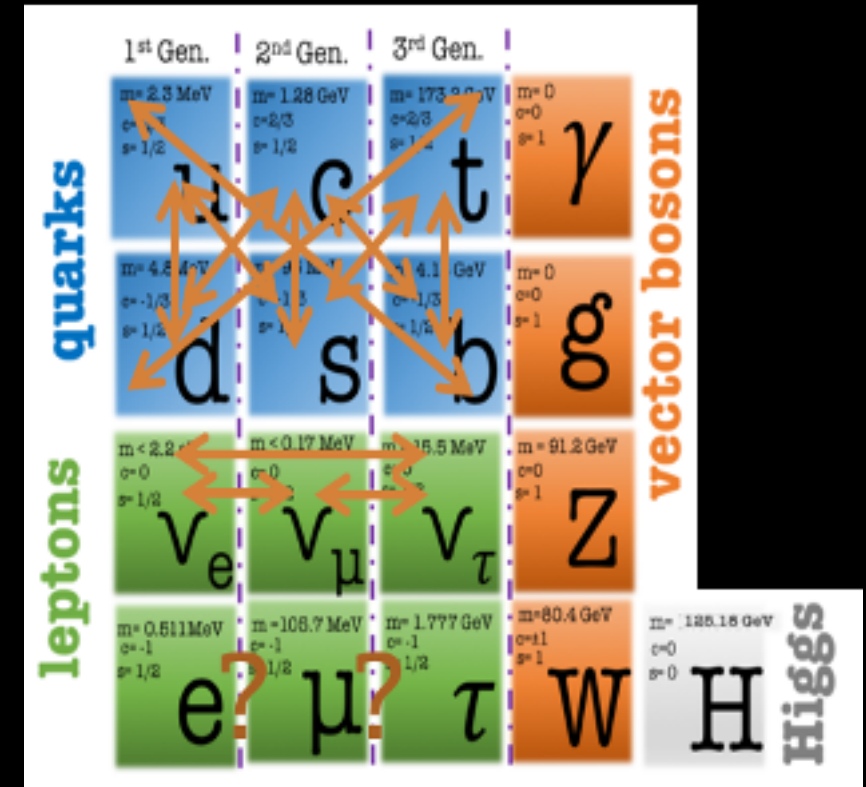
# Quark Flavor Violation



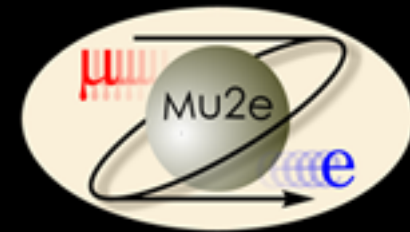
- The Quarks commit Flavor Violation
  - Mixing strengths are parameterized by **Cabibbo–Kobayashi–Maskawa (CKM)** matrix:

$$(d', s', b') = \begin{pmatrix} V_{ud} & V_{us} & V_{ub} \\ V_{cd} & V_{cs} & V_{cb} \\ V_{td} & V_{ts} & V_{tb} \end{pmatrix} \begin{pmatrix} d \\ s \\ b \end{pmatrix}$$

→ almost diagonal.



# Neutral Lepton Flavor Violations

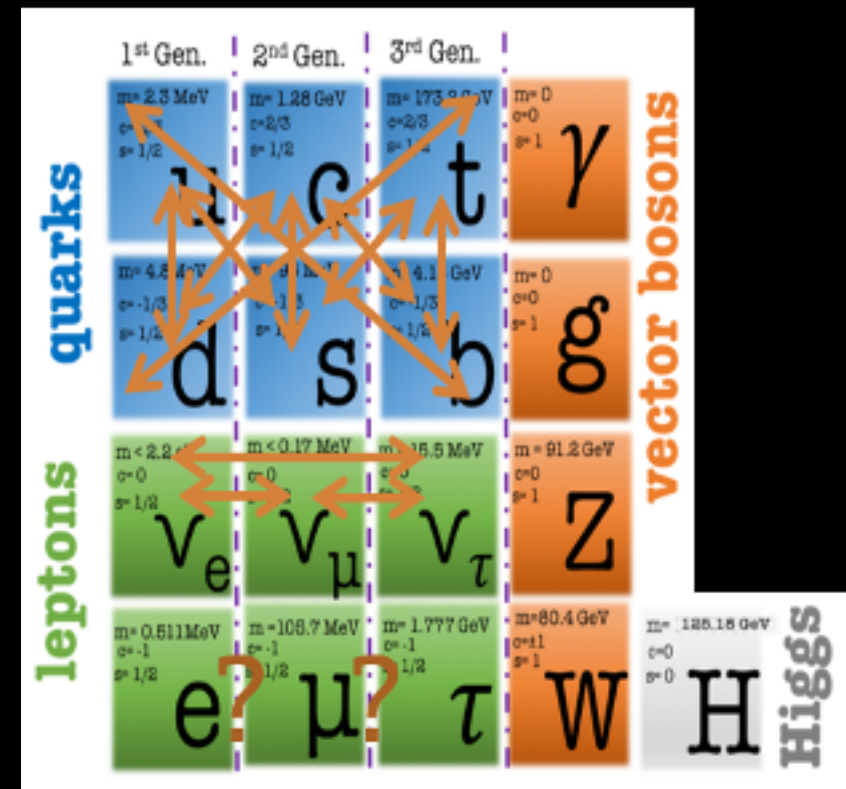


- $\nu$  oscillations  $\rightarrow$  Lepton Flavour Violation (LFV)
  - Mixing strengths parameterised by the **Pontecorvo–Maki–Nakagawa–Sakata matrix** (PMNS) matrix:

$$(\nu_e, \nu_\mu, \nu_\tau) = \begin{pmatrix} U_{e1} & U_{e2} & U_{e3} \\ U_{\mu 1} & U_{\mu 2} & U_{\mu 3} \\ U_{\tau 1} & U_{\tau 2} & U_{\tau 3} \end{pmatrix} \begin{pmatrix} \nu_1 \\ \nu_2 \\ \nu_3 \end{pmatrix}$$

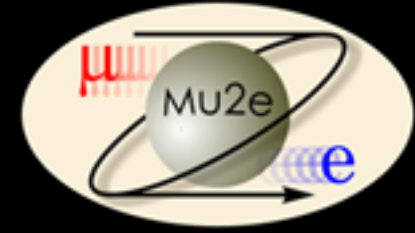
$\rightarrow$  maximal mixing

i.e. The current best fit values imply that there is much more neutrino mixing than there is mixing between the quark flavors in the CKM matrix.





# Charged Lepton Flavor Violation (CLFV)

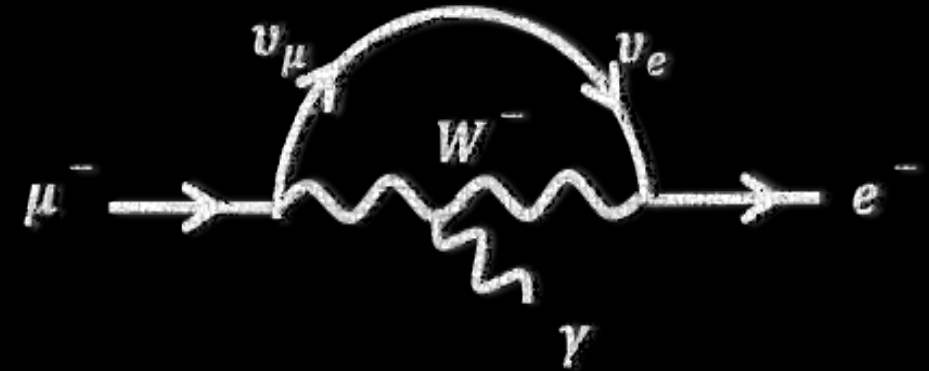


- The minimal extension of the Standard Model, including Dirac masses of neutrinos, allows for CLFV at loop level, mediated by W bosons.
- However, rates are heavily suppressed by GIM suppression and are far below any conceivable experiment could measure, for example:

$$B(\mu \rightarrow e\gamma) = \frac{3\alpha}{32\pi} \left| \sum_{i=2,3} U_{\mu i}^* U_{ei} \frac{\Delta m_{1i}^2}{M_W^2} \right|^2 \quad [1-4]$$

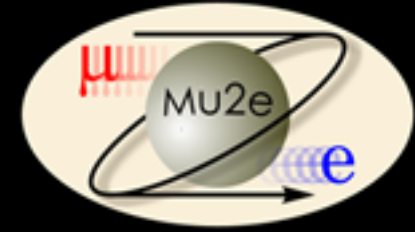
$$B(\mu \rightarrow e\gamma) = \frac{3\alpha}{32\pi} \left( \frac{1}{4} \right) \sin^2 2\theta_{13} \sin^2 \theta_{23} \left| \frac{\Delta m_{13}^2}{M_W^2} \right|^2$$

$$B(\mu \rightarrow e\gamma) \approx \mathcal{O}(10^{-54})$$



- using best-fit values for neutrino data ( $m_{\nu j}$  for the neutrino mass and  $U_{ij}$  for the element of the PMNS matrix).
- Mu2e is a search for the coherent, neutrinoless conversion of the muon to the electron in the presences of a nucleus.
- If observed, this would be an unambiguous sign of physics beyond the Standard Model (BSM).

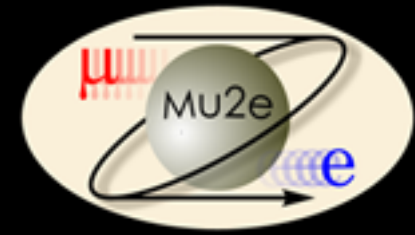
# Charged Lepton Flavor Violation (CLFV)



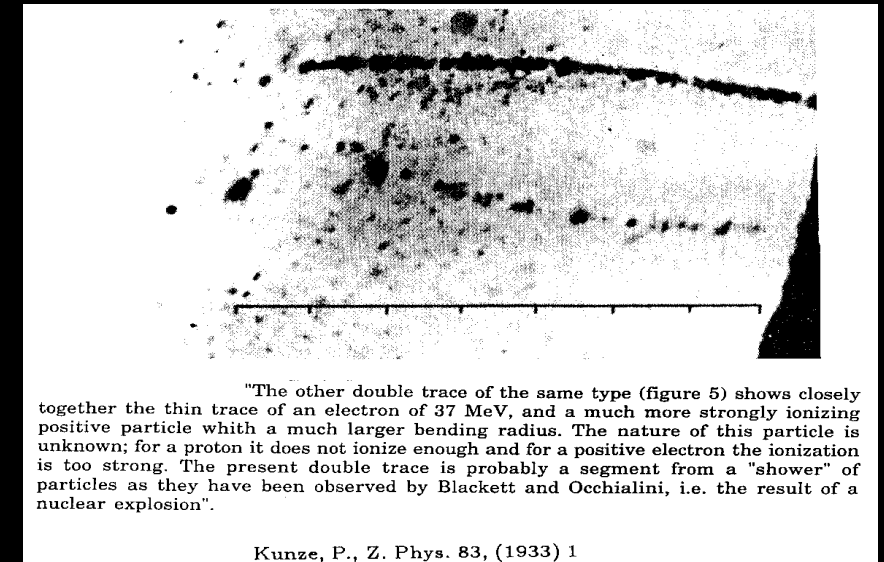
- There are many well-motivated BSM theories which invoke CLFV mediated by (pseudo) scalar, (axial) vector, or tensor currents at rates close to current experimental limits i.e.  $B \approx 10^{-15} - 10^{-17}$ .
- Some Examples (there are many others):
  - SO(10) SUSY**  
L. Calibbi *et al.*, Phys. Rev. D **74**, 116002 (2006), L. Calibbi *et al.*, JHEP **1211**, 40 (2012).
  - Scalar Leptoquarks**  
J.M. Arnold *et al.*, Phys. Rev D **88**, 035009 (2013).
  - Left-Right Symmetric Models**  
C.-H. Lee *et al.*, Phys. Rev D **88**, 093010 (2013).
  - Littlest Higgs**  
Monika Blanke, Andrzej J. Buras, Bjoern Duling, Stefan Recksiegel, Cecilia Tarantino, Acta Phys.Polon.B41:657,2010, arXiv:0906.5454v2 [hep-ph]
- Different neutrino mass-generating Lagrangians lead to very different rates of CLFV, can help explain origin of neutrino masses.

If you are interested in a detailed recent review on CLFV theory: Lorenzo Calibbi, Giovanni Signorelli arXiv:1709.00294 (2018)

# History



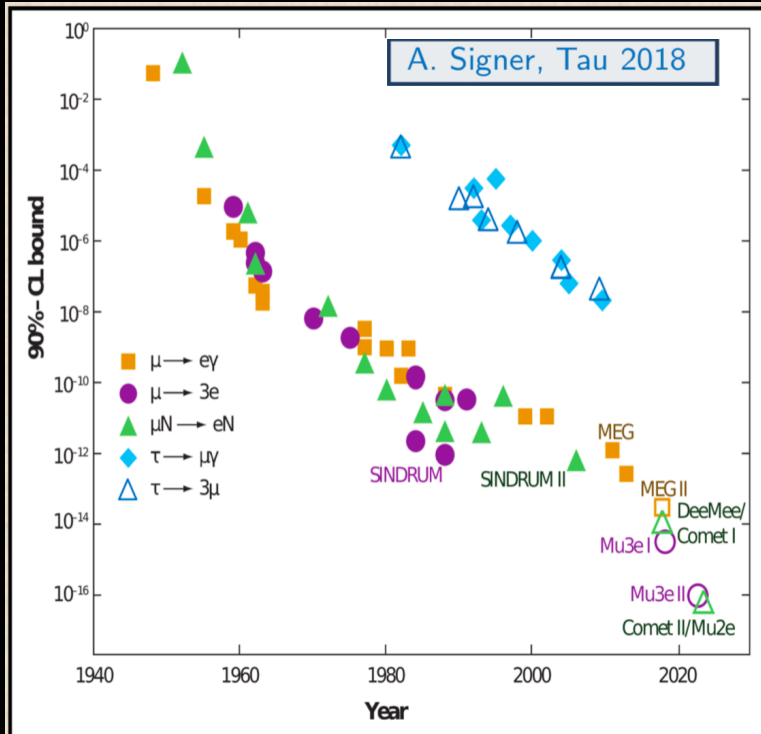
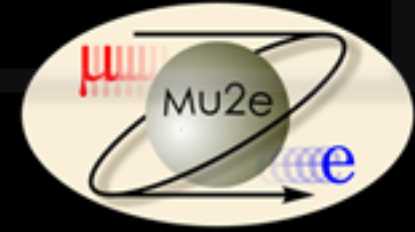
- **1933** - Kunze published first “observation” of the muon:  
*“The nature of this particle is unknown; for a proton, it does not ionize enough, and for a positive electron, the ionization is too strong”*
- **1934** - Yukawa predicts a “meson” of mass  $\sim 200m_e$  to explain the cohesion of the nucleus.
- **1936** - 3 groups independently conclude that the penetrating particle is a new one, and of intermediate mass between the electron and proton. **Neddermeyer & Anderson’s Caltech group publishes first → Discovery of the the “mu-meson”**
- **1937** - Observed that the “mu-meson” doesn’t feel the nuclear force  
**Seth H. Neddermeyer, Phys. Rev., Vol. 51, 884**
- **1948** - The muon is not an excited electron – Rabi asks “who ordered that?” muon becomes understood as heavier electron and a point-like particle. **Steinberger, J., 1948, Phys. Rev. 74 , 500.**



"The other double trace of the same type (figure 5) shows closely together the thin trace of an electron of 37 MeV, and a much more strongly ionizing positive particle with a much larger bending radius. The nature of this particle is unknown; for a proton it does not ionize enough and for a positive electron the ionization is too strong. The present double trace is probably a segment from a "shower" of particles as they have been observed by Blackett and Occhialini, i.e. the result of a nuclear explosion".

Kunze, P., Z. Phys. 83, (1933) 1

# History



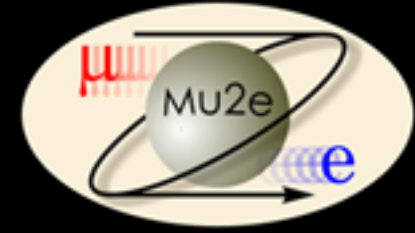
R.H. Bernstein, P.S. Cooper, Phys Rept. 532(2013)27

- 1948 - Hincks and Pontecorvo demonstrated  $\mu \rightarrow e + \gamma$  is “not a major component of the decay”. Hincks, E. P., and B. Pontecorvo (1948), Phys. Rev. 73, 257
- 1955 - J. Steinberger and Harry B. Wolfe Phys. Rev. 100, 1490. Look for electrons from muon capture – do not see any!
- 1958 - Feinberg -  $\mu \rightarrow e\gamma \sim 10^{-4-5}$  or two  $\nu$
- 2006 - SINDRUM-II finds current upper limit W. Bertl, et al. (SINDRUM-II) Eur.Phys.J. C47, 337 (2006))

- To elucidate the mechanism responsible for any CLFV – must look at relative rates in different muon channels.
- Muon-to-electron sector provides powerful probes and complements collider searches for  $\tau \rightarrow e\gamma$  or  $\mu\gamma$  and  $H \rightarrow e\tau$ ,  $\mu\tau$ , or  $\mu e$ .



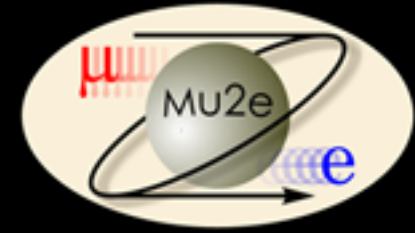
# Measuring $\mu^- N \rightarrow e^- N$



- The  $\mu \rightarrow e$  conversion rate is measured as a ratio to the muon capture rate on the same nucleus:

$$R_{\mu e} = \frac{\Gamma(\mu^- + A(Z, N) \rightarrow e^- + A(Z, N))}{\Gamma(\text{all} - \text{captures})}$$

- Low momentum (-) muons are captured in the target atomic orbit and quickly ( $\sim$ fs) cascades to 1s state.
- Muon can decay in orbit, or be captured by the nucleus, probabilities are nucleus dependent. In Al 61% captured and 39 % decay.
- The Signal:
  - Monoenergetic electron consistent with:
$$E_e = m_\mu - E_{recoil} - E_{1S B.E.}, \text{ e.g For Al: } E_e = 104.97 \text{ MeV.}$$
  - Will be smeared by detector and stopping target effects.
  - Nucleus coherently recoils off outgoing electron; it does not break-up!



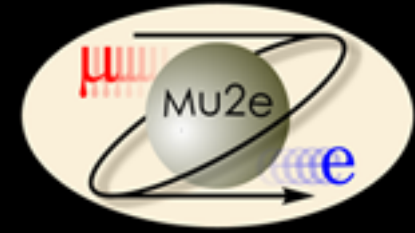
# Experimental Searches for CLFV

- The most powerful searches for CLFV use the muon state or the tau state with additional contributions from the kaon system.
- Given the high statistics available in muon beams, the muon searches have been the most powerful.
- 3 main muon-to-electron channels being looked for at facilities around the world:

| Mode                               | Current Limit (at 90% CL) | Future Proposed Limit    | Future Experiment/s |
|------------------------------------|---------------------------|--------------------------|---------------------|
| $\mu^\pm \rightarrow e^\pm \gamma$ | $5.7 \times 10^{-13}$ [5] | $4 \times 10^{-14}$      | MEG II [8]          |
| $\mu^- N \rightarrow e^- N$        | $7 \times 10^{-13}$ [6]   | $10^{-17}$               | Mu2e [9], COMET     |
| $\mu^+ \rightarrow e^+ e^+ e^-$    | $\sim 10^{-12}$ [7]       | $10^{-15} \sim 10^{-16}$ | Mu3e                |

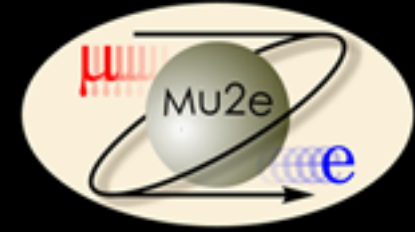
$$R_{\mu e} = \frac{\Gamma(\mu^- + A(Z, N) \rightarrow e^- + A(Z, N))}{\Gamma(\text{all} - \text{captures})} < 7 \times 10^{-13} (90\% \text{C.L.})$$

# How rare is that?



| Probability of...   |          |
|---|----------|
| rolling a 7 with two dice   | 1.67E-01 |
| rolling a 12 with two dice  | 2.78E-02 |
| getting 10 heads in a row flipping a coin   | 9.77E-04 |
| drawing a royal flush (no wild cards)   | 1.54E-06 |
| getting struck by lightning in one year in the US   | 2.00E-06 |
| winning Pick-5  | 5.41E-08 |
| winning MEGA-millions lottery (5 numbers+megaball)  | 3.86E-09 |
| your house getting hit by a meteorite this year   | 2.28E-10 |
| drawing two royal flushes in a row (fresh decks)  | 2.37E-12 |
| your house getting hit by a meteorite today   | 6.24E-13 |
| getting 53 heads in a row flipping a coin   | 1.11E-16 |
| your house getting hit by a meteorite AND you being struck by lightning both within the next six months   | 1.14E-16 |
| your house getting hit by a meteorite AND you being struck by lightning both within the next three months | 2.85E-17 |

# Indirect .v. Direct Searches



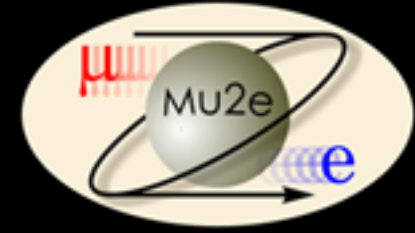
- If a signal is observed at Mu2e then this must be BSM physics – the experiment offers a deep, indirect probe for New Physics.

| Direct  | Indirect   |
|---|--|
| Produce <u>NEW PARTICLES</u> at a collider                                      | Looks for the <u>EFFECTS</u> of the new physics  |
| When we know <u>WHAT</u> we are looking for and what we want to <u>DISCOVER</u> | No need to know details of model producing new physics                                   |
| Only works if new particles are <u>WITHIN ENERGY REACH</u>                      | <u>Can still give valuable information about new particles outside our energy reach.</u> |

- Indirect searches are precision searches looking for some sign of BSM – we can use Effective Field Theories to think about the physics we might “see” at Mu2e.



# Effective Field Theory



- Extend the SM Lagrangian with higher-dimensional gauge-invariant operators that only involve the SM fields:

$$\mathcal{L} = \mathcal{L}_{SM} + \frac{1}{\Lambda} \sum_a C_a^{(5)} Q_a^{(5)} + \frac{1}{\Lambda^2} \sum_a C_a^{(6)} Q_a^{(6)} + \dots$$

- Non-renormalizable operators  $Q_a$  are noted with their dimensions.
- The coefficients  $C_a$  are dimensionless containing information about the underlying theory, and  $\Lambda \gg v$  is the cut-off of this effective field theory.
- The  $D = 5$  operators represent those which generate Majorana mass terms and these have negligible rates.
- The  $D = 6$  operators can induce CLFV processes either directly or at loop level.
- Operators may not be independent due to radiative effect.

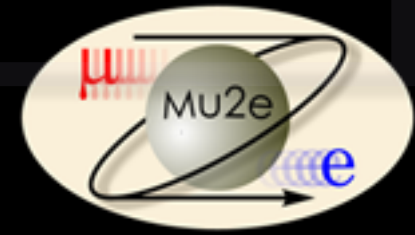
For Theoretical Overviews:

Eur. Phys. J C75 (2015) no.12, 579

V. Cirigliano, R. Kitano, Y. Okada, and P. Tuzon, Phys. Rev. D **80**, 013002 (2009)

# Simplistic Explanation of Physics Reach

Taken from A. de Gouvêa, P. Vogel  
arXiv:1303.4097



- For the purposes of discussion we can build a Toy Lagrangian which consists of 2 terms representing 2 types of physics process:

$$\mathcal{L}_{CLFV} = \frac{m_\mu}{(1+\kappa)\Lambda^2} \bar{\mu}_R \sigma_{\mu\nu} e_L F^{\mu\nu} + \frac{\kappa}{(1+\kappa)\Lambda^2} \bar{\mu}_L \gamma_\mu e_L \left( \sum_{q=u,d} \bar{q}_L \gamma_\mu q_L \right)$$

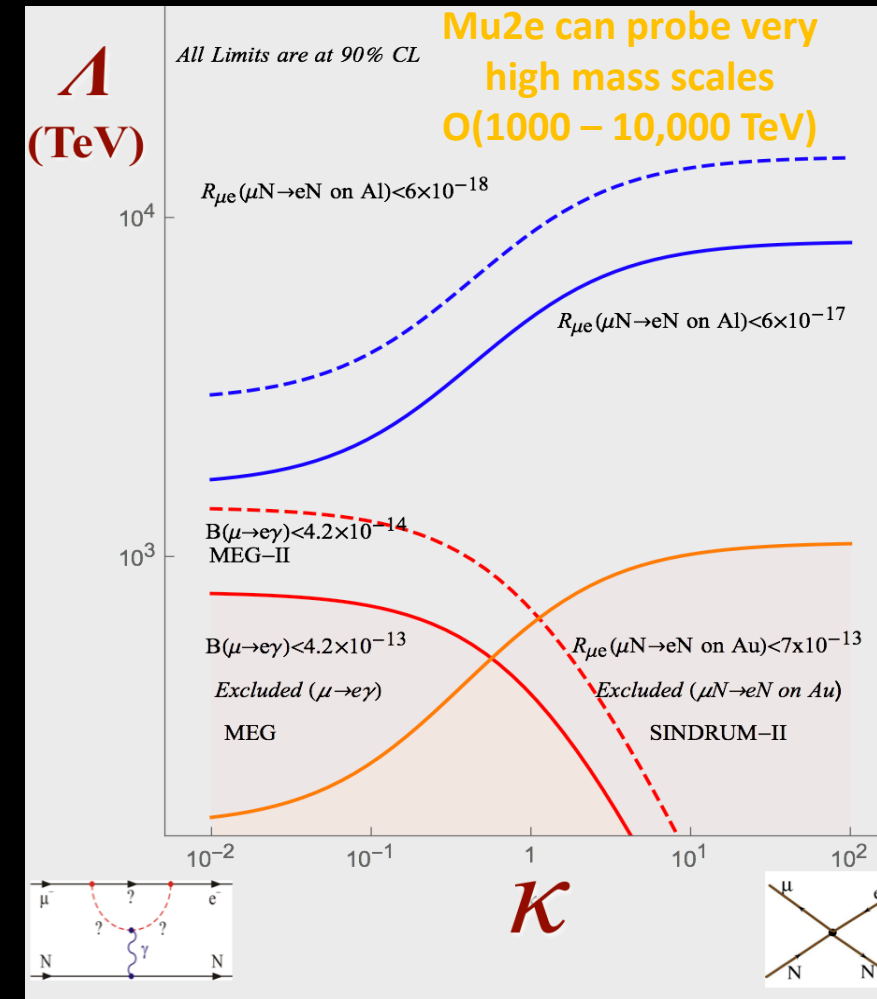
**“Photonic”**

i.e. Dipole terms:  
 $\mu^\pm \rightarrow e^\pm \gamma, \mu \rightarrow eee$   
 $\mu^- N \rightarrow e^- N$

**“Contact”**

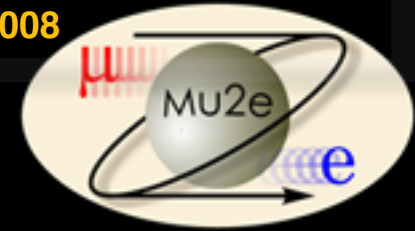
i.e. 4 fermion terms  
Only  $\mu^+ \rightarrow e^+ e^+ e^-$   
And  $\mu^- N \rightarrow e^- N$

$\lambda$  = the effective mass scale of new physics (NP),  
 $\kappa$  = determines to what extent NP is photonic ( $=0$ )  
or 4-fermion ( $=\infty$ )



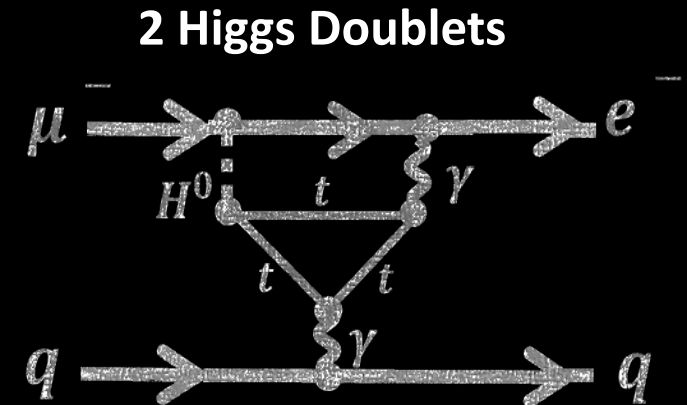
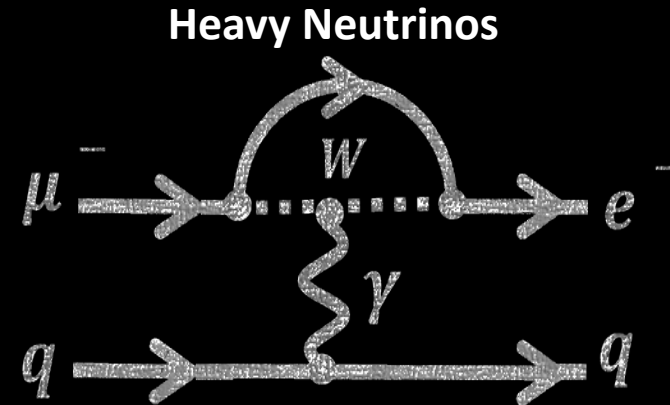
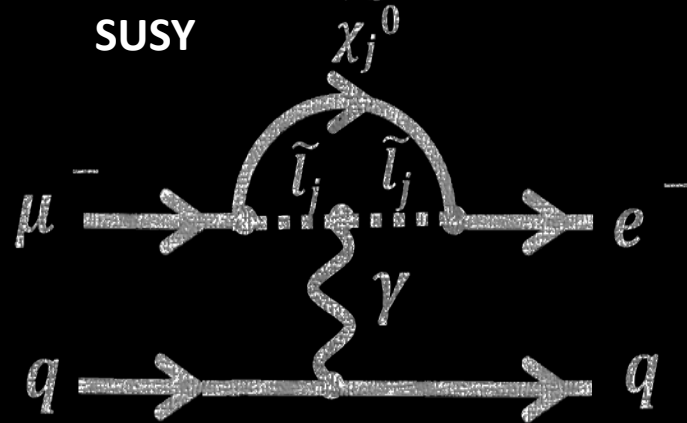
# Physics Reach

Theory Reviews: Y. Kuno, Y. Okada, 2001; M. Raidal et al., 2008  
A. de Gouvêa, P. Vogel, 2013



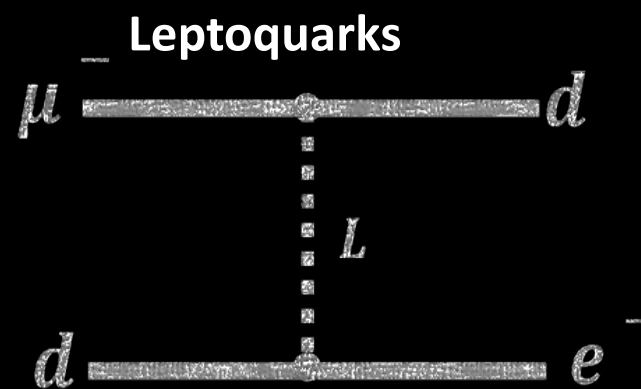
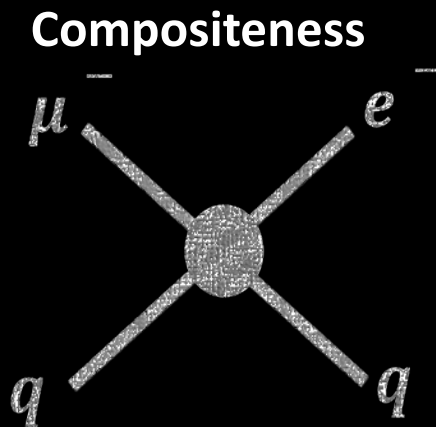
Multitude of possible new physics contributions to  $\mu N \rightarrow e N$  which predict  $R_{\mu e} \sim O(10^{-15})$  i.e.  $\sim 40$  Mu2e events

**Loop  
“Photonic”**

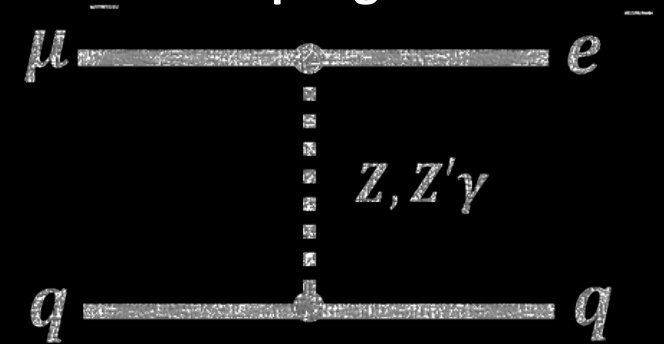


Sensitive to mass scales up to  $O(10^4 \text{ TeV})$

**“Contact”**

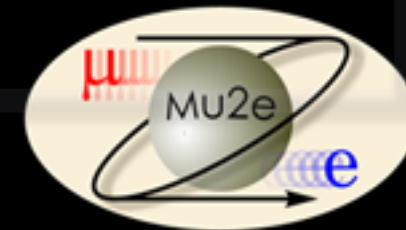


**Anomalous Couplings**



# Physics Reach

Table 8: “DNA” of flavour physics effects for the most interesting observables in a selection of SUSY and non-SUSY models ★★★ signals large effects, ★★ visible but small effects and ★ implies that the given model does not predict sizable effects in that observable.



Taken from: arXiv:0909.1333[hep-ph]

Discovery sensitivity across the board.  
Relative Rates however will be model dependent.

| Model           | $\mu \rightarrow eee$ | $\mu N \rightarrow eN$ | $\frac{\text{BR}(\mu \rightarrow eee)}{\text{BR}(\mu \rightarrow e\gamma)}$ | $\frac{\text{CR}(\mu N \rightarrow eN)}{\text{BR}(\mu \rightarrow e\gamma)}$ |
|-----------------|-----------------------|------------------------|---|--|
| MSSM            | Loop                  | Loop                   | $\approx 6 \times 10^{-3}$  | $10^{-3} - 10^{-2}$  |
| Type-I seesaw   | Loop*                 | Loop*                  | $3 \times 10^{-3} - 0.3$  | $0.1 - 10$   |
| Type-II seesaw  | Tree                  | Loop                   | $(0.1 - 3) \times 10^3$   | $\mathcal{O}(10^{-2})$   |
| Type-III seesaw | Tree                  | Tree                   | $\approx 10^3$  | $\mathcal{O}(10^3)$  |
| LFV Higgs       | Loop†                 | Loop*†                 | $\approx 10^{-2}$   | $\mathcal{O}(0.1)$   |
| Composite Higgs | Loop*                 | Loop*                  | $0.05 - 0.5$  | $2 - 20$   |

from L. Calibbi and G. Signorelli, Riv. Nuovo Cimento, 41 (2018) 71

|  | AC  | RVV2 | AKM | $\delta$ LL | FBMSSM | LHT | RS  |
|--|-----|------|-----|-------------|--------|-----|-----|
| $D^0 - \bar{D}^0$                        | ★★★ | ★    | ★   | ★           | ★      | ★★★ | ?   |
| $\epsilon_K$                             | ★   | ★★★  | ★★★ | ★           | ★      | ★★  | ★★★ |
| $S_{\psi\phi}$                           | ★★★ | ★★★  | ★★★ | ★           | ★      | ★★★ | ★★★ |
| $S_{\phi K_S}$                           | ★★★ | ★★   | ★   | ★★★         | ★★★    | ★   | ?   |
| $A_{CP}(B \rightarrow X_s \gamma)$       | ★   | ★    | ★   | ★★★         | ★★★    | ★   | ?   |
| $A_{7,8}(B \rightarrow K^* \mu^+ \mu^-)$ | ★   | ★    | ★   | ★★★         | ★★★    | ★★  | ?   |
| $A_9(B \rightarrow K^* \mu^+ \mu^-)$     | ★   | ★    | ★   | ★           | ★      | ★   | ?   |
| $B \rightarrow K^{(*)} \nu \bar{\nu}$    | ★   | ★    | ★   | ★           | ★      | ★   | ★   |
| $B_s \rightarrow \mu^+ \mu^-$            | ★★★ | ★★★  | ★★★ | ★★★         | ★★★    | ★   | ★   |
| $K^+ \rightarrow \pi^+ \nu \bar{\nu}$    | ★   | ★    | ★   | ★           | ★      | ★★★ | ★★★ |
| $K_L \rightarrow \pi^0 \nu \bar{\nu}$    | ★   | ★    | ★   | ★           | ★      | ★★★ | ★★★ |
| $\mu \rightarrow e \gamma$               | ★★★ | ★★★  | ★★★ | ★★★         | ★★★    | ★★★ | ★★★ |
| $\tau \rightarrow \mu \gamma$            | ★★★ | ★★★  | ★   | ★★★         | ★★★    | ★★★ | ★★★ |
| $\mu + N \rightarrow e + N$              | ★★★ | ★★★  | ★★★ | ★★★         | ★★★    | ★★★ | ★★★ |

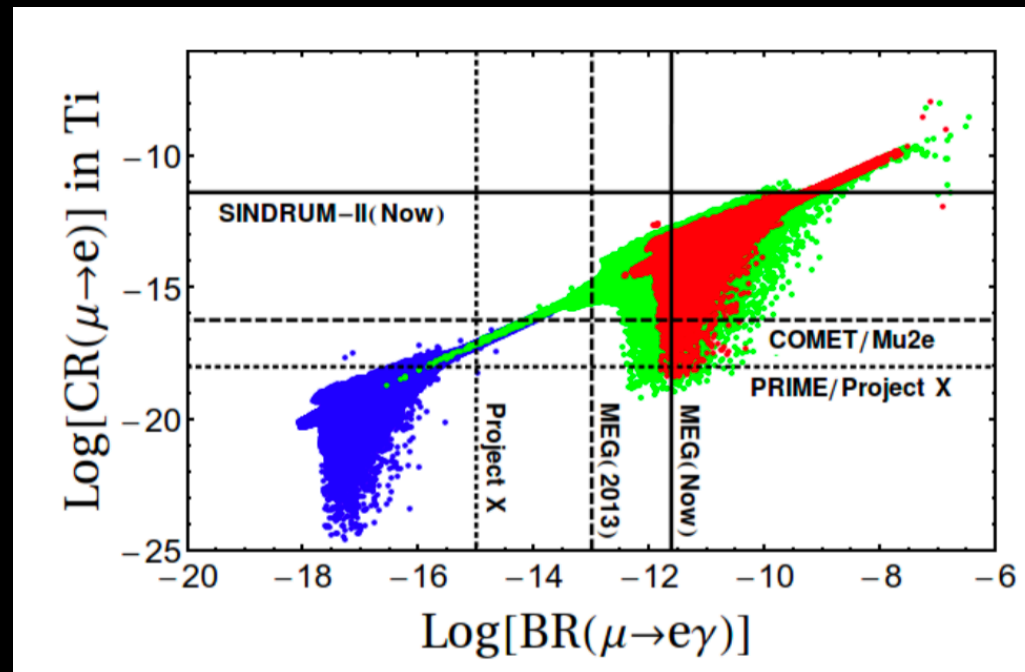
★★★ = Discovery Sensitivity



# Physics Reach

**Top:** Shows SUSY models with  $\tan\beta = 10$  for various possible CLFV matrices the PMNS case in mSUGRA (red) and NUHM (green), and for the CKM case (blue)

L. Calibbi et al., JHEP 1211 (2012) 040



L. Calibbi, G. Signorelli arXiv:1709.00294

If we see a signal – which line is it consistent with?  
Can help constrain SUSY models.

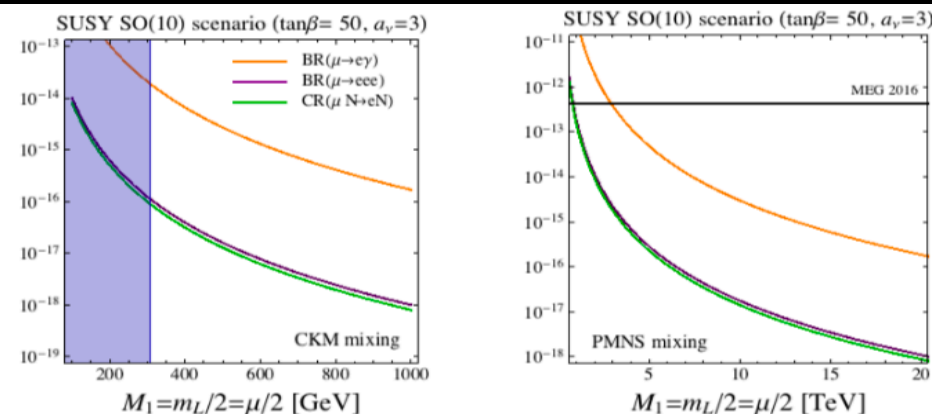
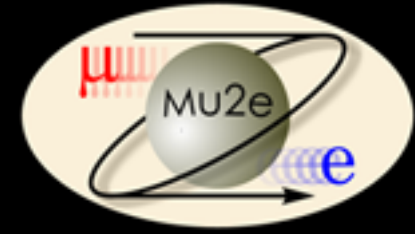


Figure 11. – Left: Rates of  $\mu \rightarrow e$  processes as predicted in a SUSY seesaw with the ‘minimal’  $SO(10)$  relation in Eq. (56).  $SO(10)$  mass relations among SUSY particles are taken. The blue-shaded area is excluded by the latest searches for gluinos at the LHC [129, 130]. The chosen parameters aim at maximising the CLFV effects, e.g.  $BR(\mu \rightarrow e\gamma) \propto (3 + a_\nu)^2 \tan^2 \beta$ . Right: the same for the case of  $SO(10)$  with large slepton mixing as given by Eq. (59).

# Physics Reach



J.M. Arnold *et al.*, Phys. Rev D **88**, 035009 (2013).

- Scalar Leptoquarks:
  - Models with scalar leptoquarks at the TeV scale can, through top mass enhancement, modify the  $\mu \rightarrow e$  conversion rate and  $\text{BR}(\mu \rightarrow e\gamma)$  while satisfying all known experimental constraints from collider and quark flavor physics.
  - Couplings constrained by measuring BR of muon-to-electron conversion.

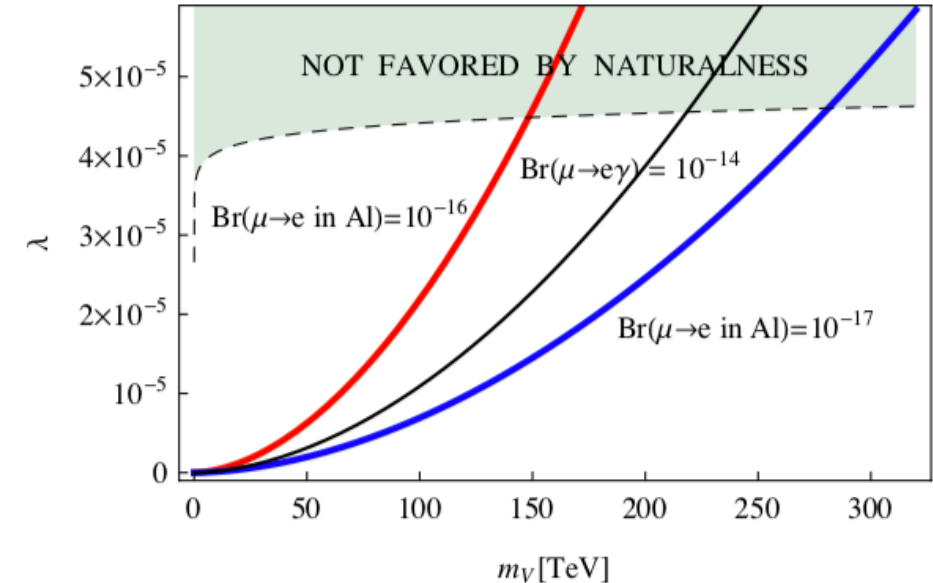
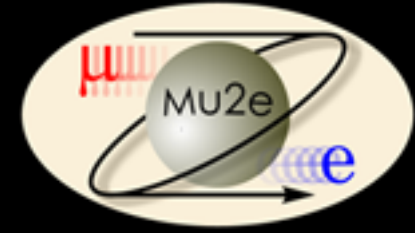
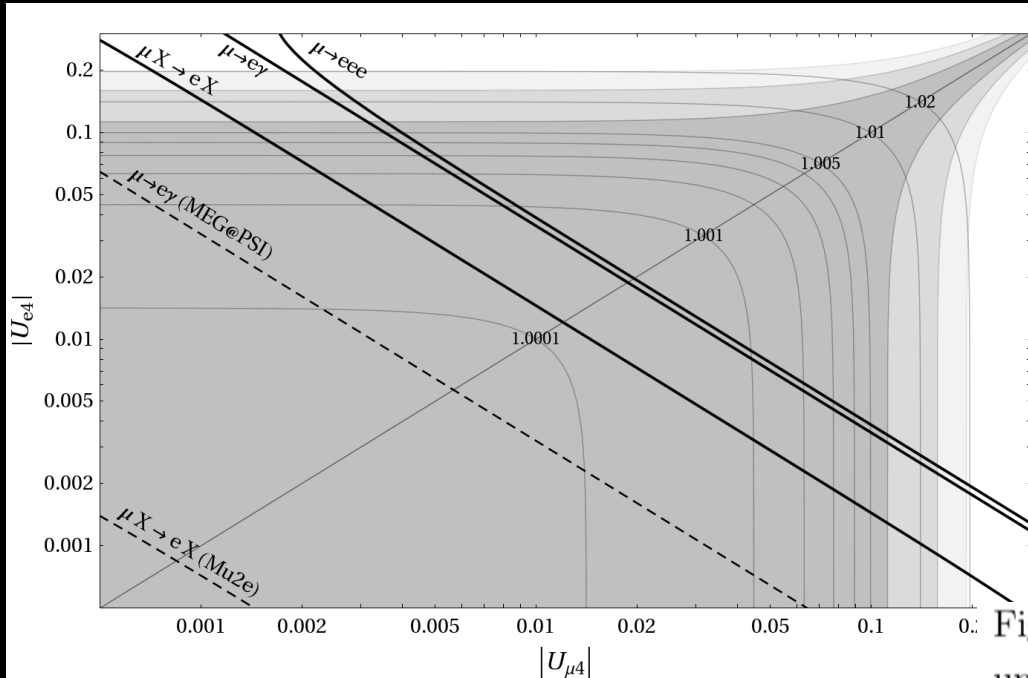


FIG. 3: The combination of couplings  $\lambda$  from Eq. (14) as a function of the scalar leptoquark mass for two values of the  $\text{Br}(\mu \rightarrow e \text{ in Al})$  relevant for the Mu2e experiment. The thin solid line, corresponding to  $\text{Br}(\mu \rightarrow e\gamma) = 10^{-14}$ , is included for reference. The shaded region consists of points which do not satisfy Eq. (7).

# Physics Reach



- Constraining Sterile neutrinos:



$U_{L4}$  – the SM-4 PMNS extension element for the 4<sup>th</sup> generation neutrino and the L lepton

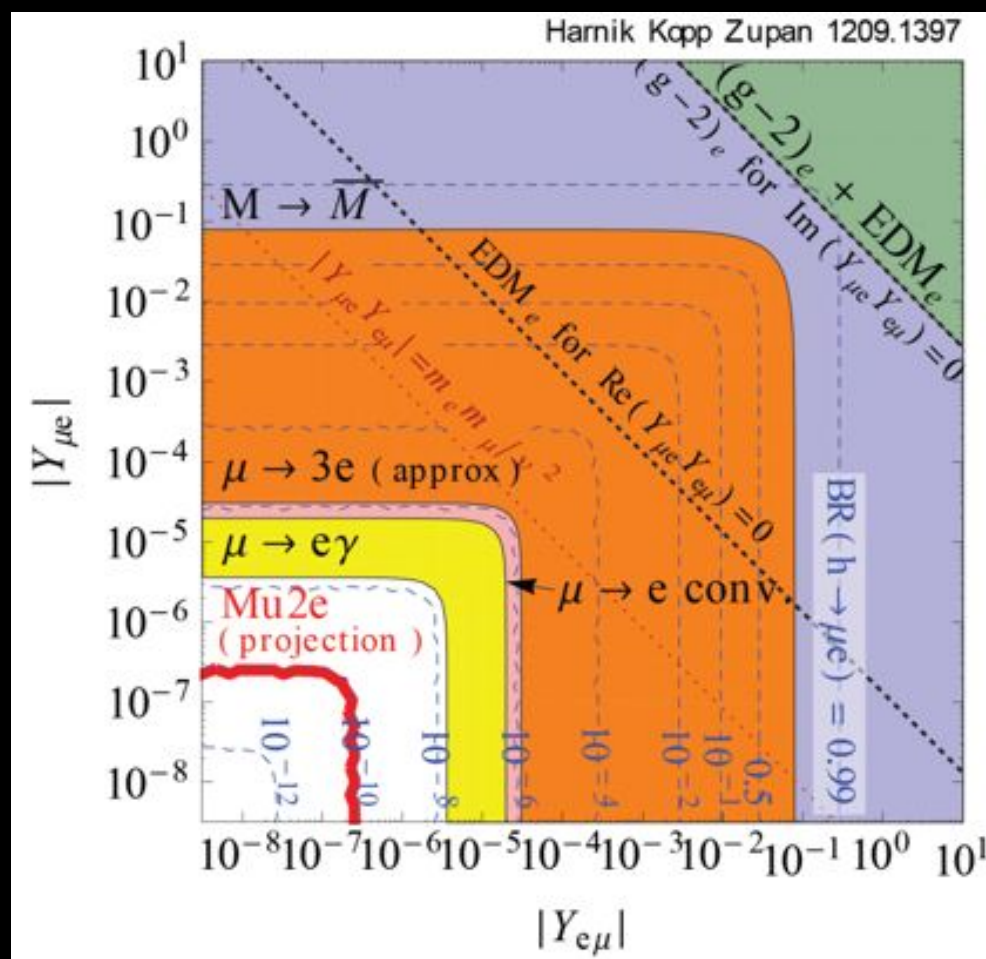
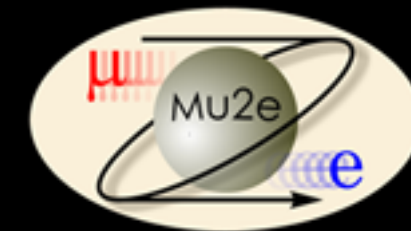
Many BSM theories which predict heavy neutral leptons allow for higher rates of LFV.

LFV measurements can help constrain BSM models which predict heavy neutral leptons.

Buras, Duling, Feldmann, Heidsieck, Promberger, 1006.5356

Figure 5: Constraints on the allowed range of  $|U_{e4}|$  and  $|U_{\mu 4}|$  resulting from lepton universality ( $1\sigma/2\sigma/3\sigma$ : dark gray/gray/light gray area, respectively) and the current experimental bounds on  $\mu \rightarrow eee$ ,  $\mu \rightarrow e\gamma$ , and  $\mu - e$  conversion (thick black lines). The contour lines indicate the ratio  $G_F^{SM4}/G_F^{SM3}$ , where  $G_F^{SM4}$  is the value of the Fermi constant extracted from muon lifetime measurement assuming 4 generations, and  $G_F^{SM3}$  is the usual SM3 Fermi constant (s. [16]).

# Constraining Flavor Violating Higgs Decays



- Can also help constrain flavor violating Higgs decays  
Harnik, J. Kopp and J. Zupan, JHEP **3**, 26 (2013).

- Current  $\mu \rightarrow e$  conversion implies:

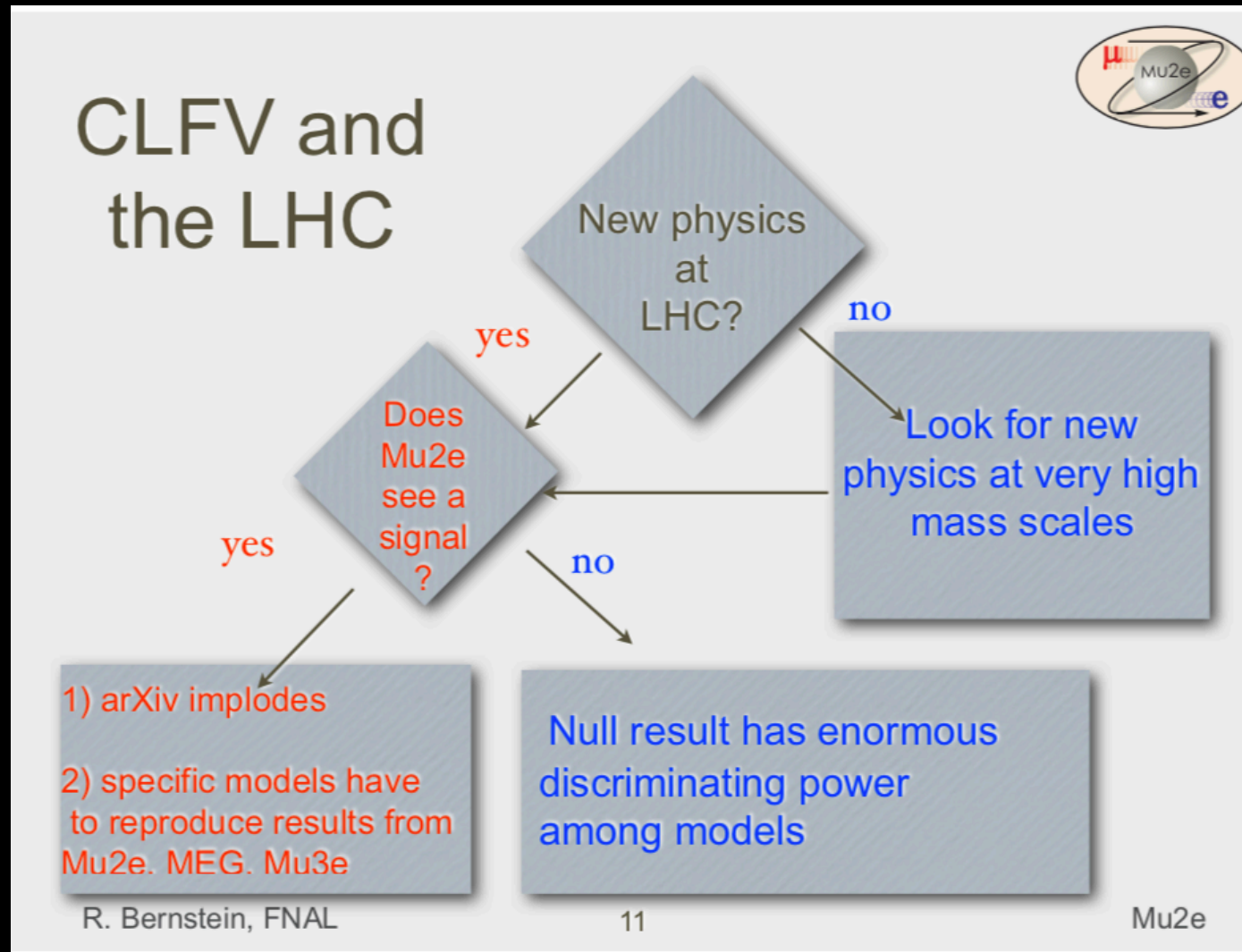
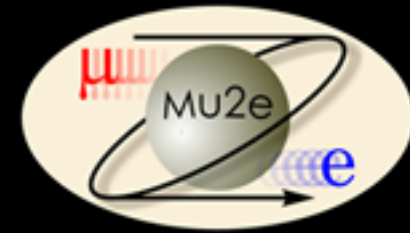
$$\sqrt{|Y_{\mu e}|^2 + |Y_{e\mu}|^2} < 4.6 \times 10^{-5}$$

- Mu2e is expected to be sensitive to:

$$\sqrt{|Y_{\mu e}|^2 + |Y_{e\mu}|^2} > \text{few} \times 10^{-7}.$$

- Where  $|Y_{\mu e}|$  and  $|Y_{e\mu}|$  are flavor-violating Yukawa couplings for a 125 GeV Higgs boson i.e.  $h \rightarrow \mu e$ .
- In these types of scenarios, constraints involving muon  $\mu e$ ,  $e\mu$  couplings are substantially stronger than those involving  $\tau$  couplings.

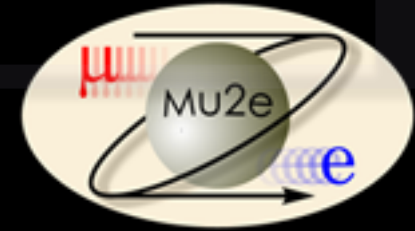
# Possibilities





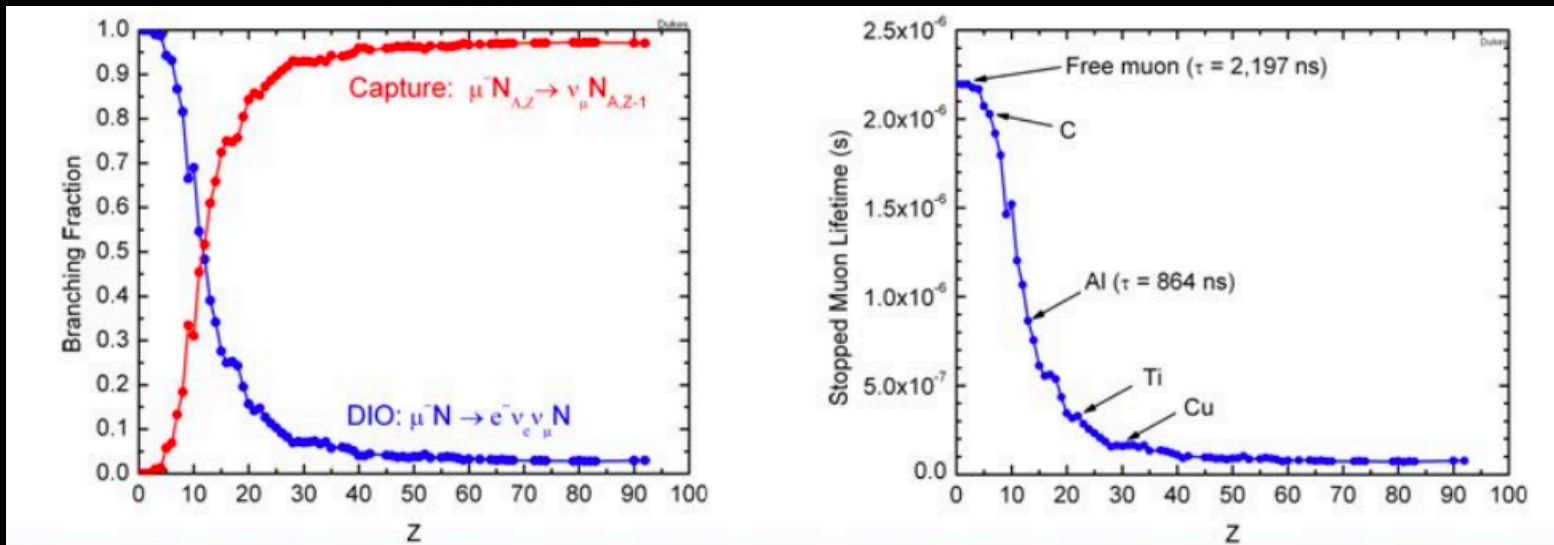
# Why Aluminum?

For more information about target nuclei: [arxiv.org/abs/hep-ph/0203110v4](https://arxiv.org/abs/hep-ph/0203110v4)



- Target material must be chemically stable and available in the required size, shape, and thickness.
- Conversion energy such that only tiny fraction of photons produced by muon radiative capture.
- Muon lifetime long compared to transit time of prompt backgrounds.
- Conversion rate increases with atomic number, reaching maximum at Se and Sb, then drops. Lifetime of muonic atoms decreases with increasing atomic number.

→ Al (or Ti) best choices for Mu2e.



The lifetime of a muon in a muonic atom decreases with increasing atomic number.



# What happens if we see a signal?



V. Cirigliano, S. Davidson, YK, Phys. Lett. B 771 (2017) 242  
S. Davidson, YK, A. Saporta, Eur. Phys. J. C78 (2018) 109

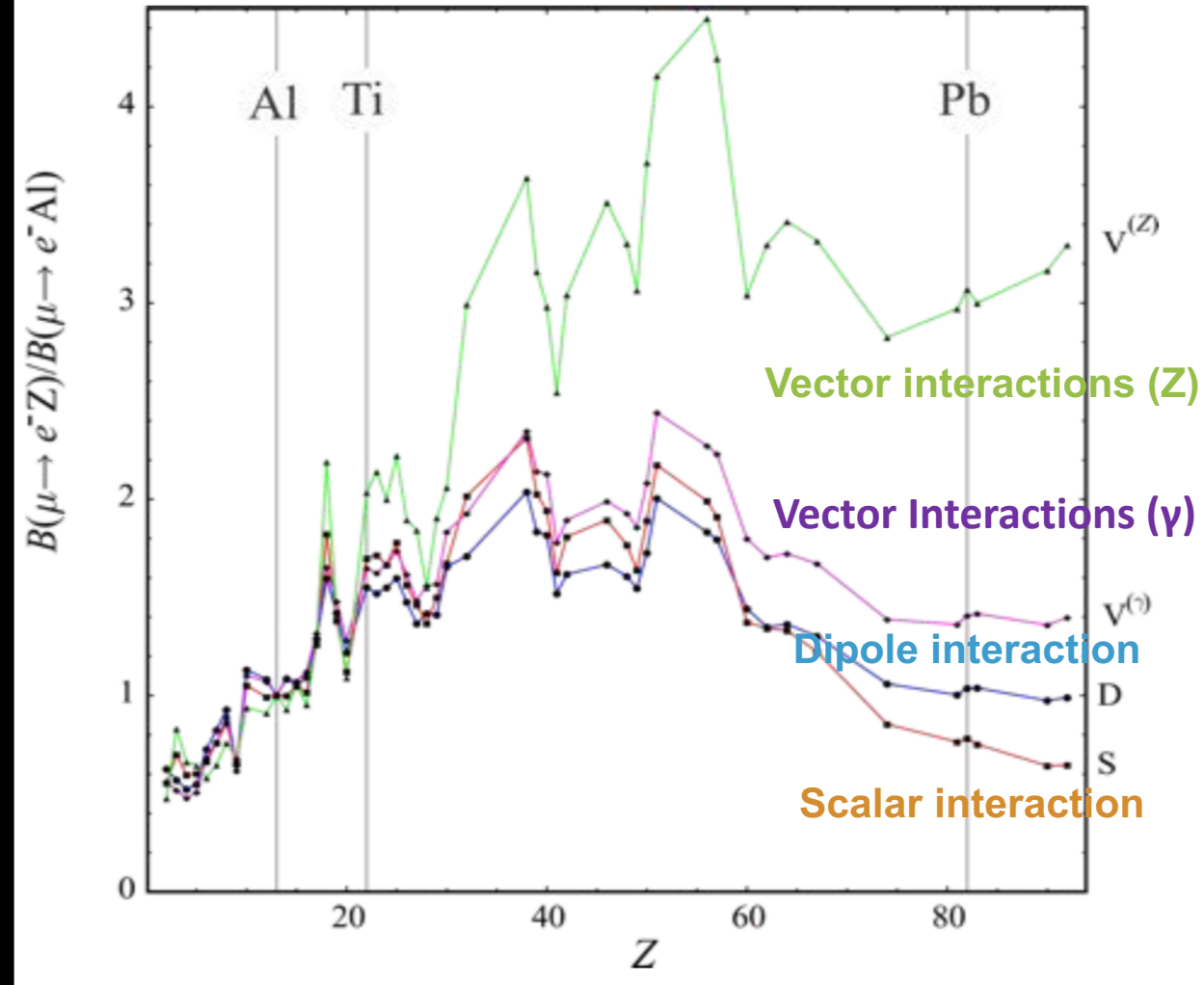
If we do see a signal in Al:

- Various operator coefficients add coherently in the amplitude.
  - Weighted by nucleus-dependent functions.
- Requires measurements of conversion rate in other target materials!

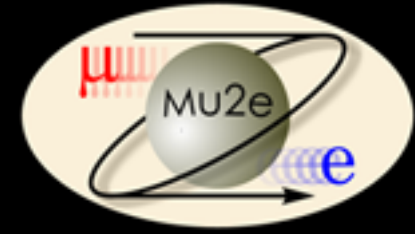
|   | S                        | D    | V <sup>1</sup> | V <sup>2</sup>           |
|---|--------------------------|------|----------------|--------------------------|
| $\frac{B(\mu \rightarrow e, \text{Ti})}{B(\mu \rightarrow e, \text{Al})}$ | $1.70 \pm 0.005_y$       | 1.55 | 1.65           | 2.0                      |
| $\frac{B(\mu \rightarrow e, \text{Pb})}{B(\mu \rightarrow e, \text{Al})}$ | $0.69 \pm 0.02_{\rho_n}$ | 1.04 | 1.41           | $2.67 \pm 0.06_{\rho_n}$ |

$y$  = nuclear scalar form factor,  $\rho_n$  = nuclear neutron density

5% measurement on Al/Ti needed to see split

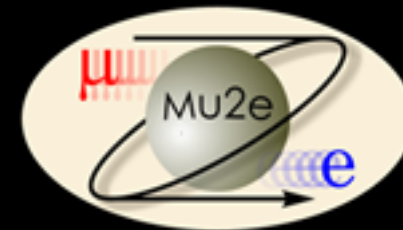


# Sindrum-II: How can we improve on this?



- The SINDRUM-II results was limited by 2 main factors:
  1. Backgrounds from prompt pions,
  2. The muon stopping rate ( $\sim 10^7 \mu/s$  -with a  $\sim 1$  MW beam).
- Mu2e must address these issues to improve limit on  $R_{\mu e}$ .
- Following the proposal by V. Lobashev & R. Djilkibaev (Sov. J. Nucl. Phys. 49(2), 384 (1989)) , Mu2e will:
  - Utilize a pulsed proton beam & delayed “gate window”
    - Eliminates pion induced backgrounds.
  - Use intense muon source
    - $10^{10}$  muons/s.
  - Use superconducting solenoids
    - For efficient muon collection and transport to stopping target.

Mu2e aims to achieve  $3 \times 10^{20}$  POT over a number of years, starting in 2024



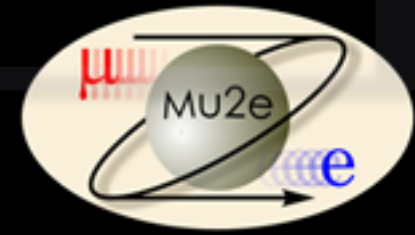
# Removing Backgrounds

Beam delivery and detector systems optimized for high intensity, pure muon beam – must be “background free”:

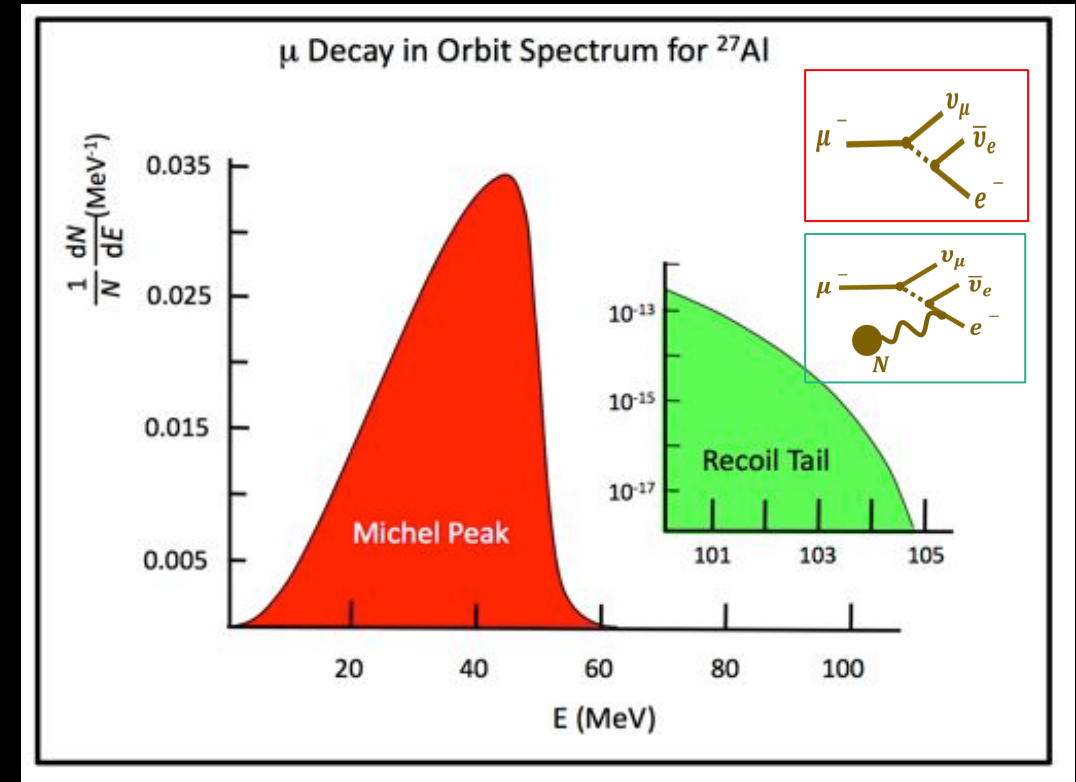
- Intrinsic :
  - Scale with number of stopped muons.
- Late arriving :
  - Scale with number of late protons/ extinction performance

| Type          | Source               | Mitigation         | Yield                                       |
|---------------|----------------------|--------------------|---|
| Intrinsic     | Decay in Orbit (DIO) | Tracker Resolution | $0.144 \pm 0.028$ (stat) $\pm 0.11$ (sys)   |
| Late Arriving | Pion Capture         | Beam Structure     | $0.021 \pm 0.001$ (stat) $\pm 0.002$ (sys)  |
|               | Pion Decay in Flight | -                  | $0.001 \pm < 0.001$                         |
| Other         | Anti-proton          | Thin windows       | $0.04 \pm 0.022$ (stat) $\pm 0.020$ (sys)   |
|               | Cosmic Rays          | Veto System        | $0.209 \pm 0.0022$ (stat) $\pm 0.055$ (sys) |

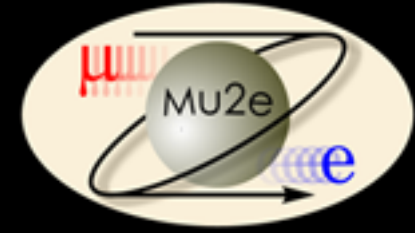
# Muon Decay-in-Orbit



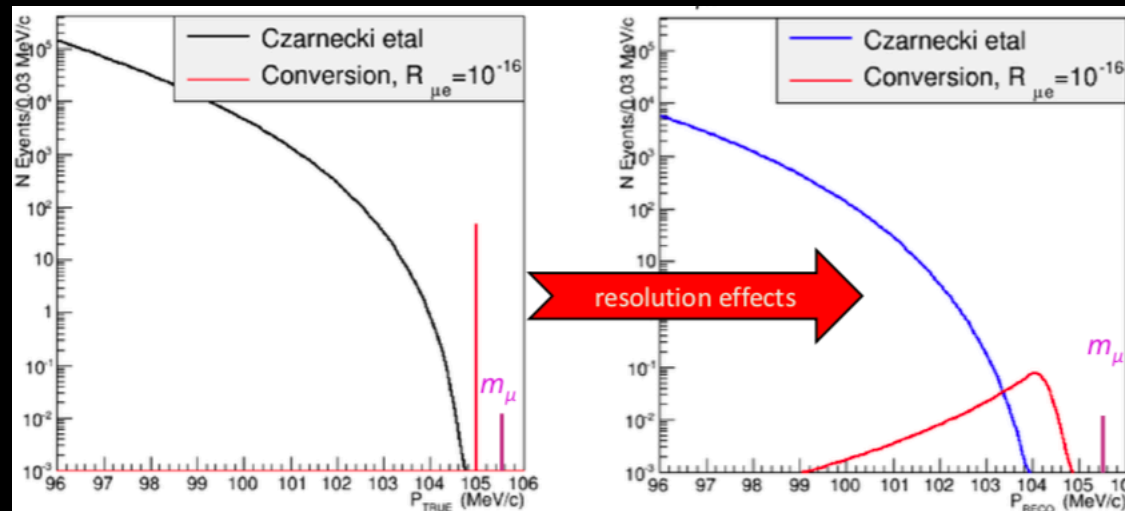
- In Aluminium 39% of stopped muons will decay in orbit (DIO).
- Free muon decay: peak electron energy far below our signal energy (peaks 52.8 MeV).
- If muon is bound in atomic orbit, the outgoing electron can exchange momentum with the nucleus.
- Small probability that an electron with energy close to that of a conversion electron can be produced.
- The differential energy spectrum of DIO electron spectrum has been parameterized in A. Czarnecki et al., "Muon decay in orbit: Spectrum of high-energy electrons," Phys. Rev. D 84 (Jul, 2011) .



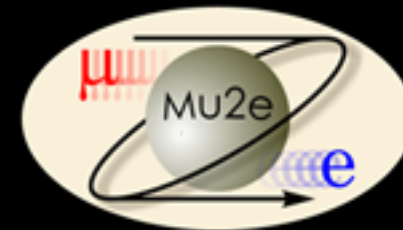
# Muon Decay-in-Orbit



- The muon DIO spectrum decreases near the endpoint as  $(E - E_{MAX})^5$  and within the last MeV its probability is below  $10^{-16}$ .
- Detector Resolution effects and effects of scattering in the stopping target can extend the DIO endpoint into the signal region
- **Necessitates tracker resolution of  $< 200$  KeV/c**



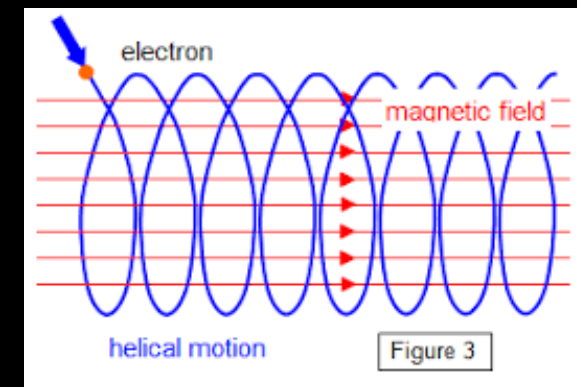
# Rejecting DIO



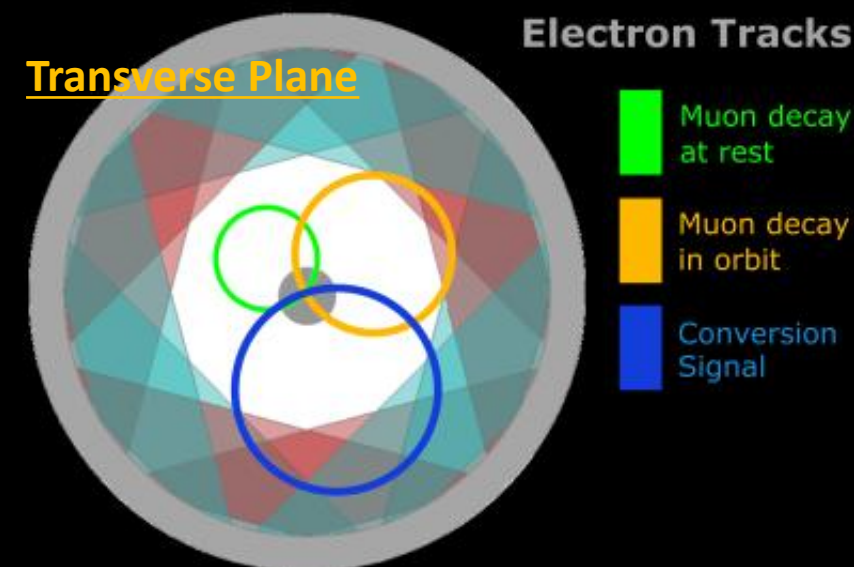
- Charged particle traverses a solenoidal field it follows a helical path.
- The radius of the helix is determined by the magnetic field and the particle momentum i.e. conversion electron of  $p \sim 105 \text{ MeV}/c$ , in a 1 T field:

$$R = \frac{p_{\perp}}{qB} = 35 \text{ cm}$$

- Mu2e employs track reconstruction algorithms and Kalman Filtering.
- Momentum resolution  $\sim 180 \text{ KeV}/c$ .

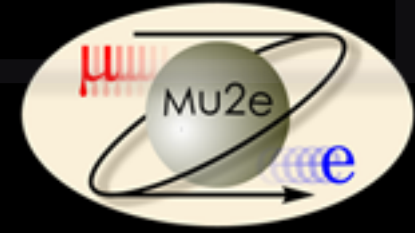


## Transverse Plane



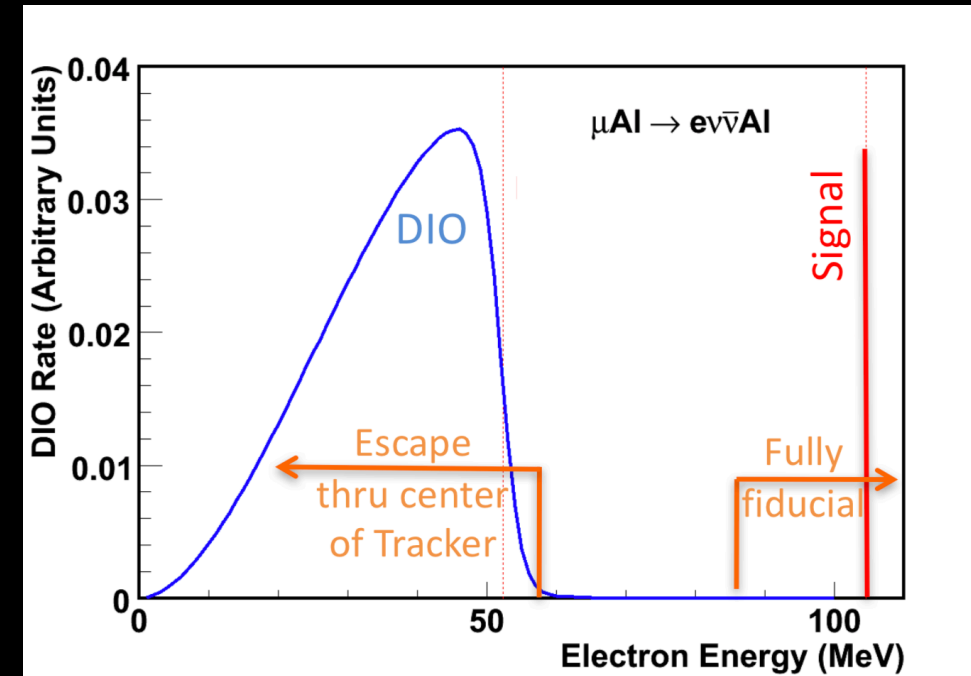


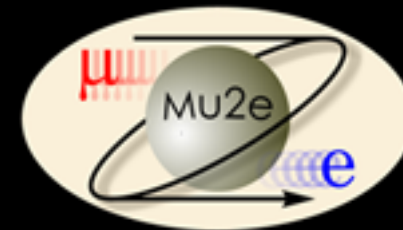
# Rejecting DIO



A low mass, annular, highly segmented detector is used to:

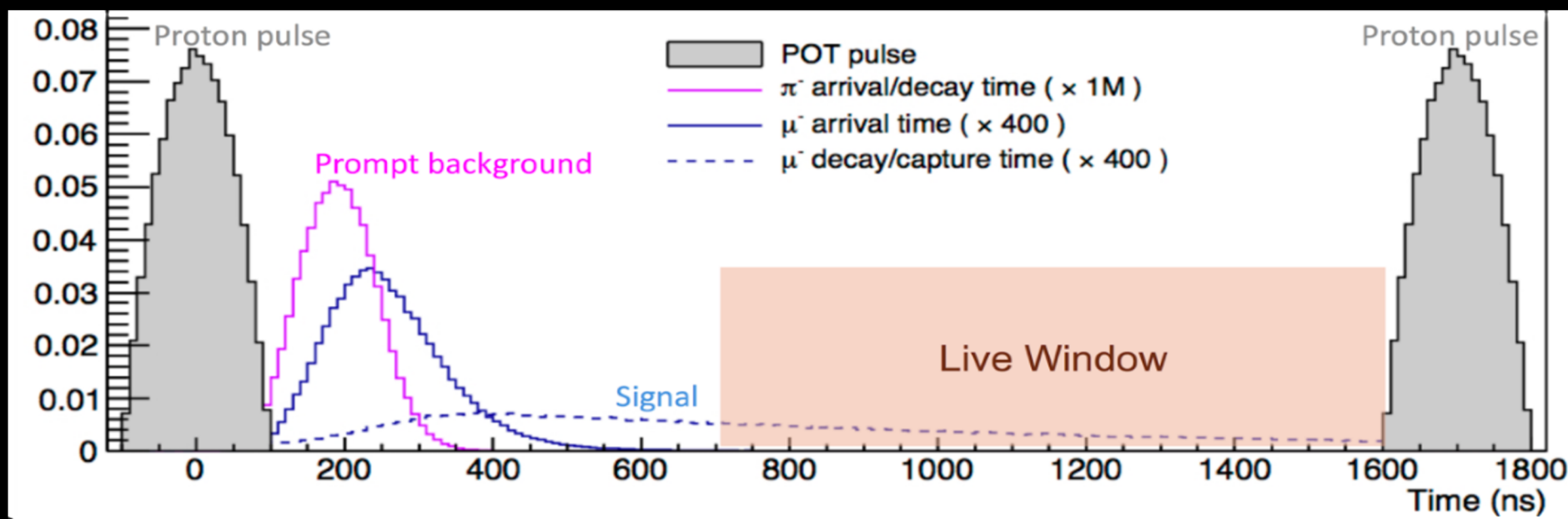
1. **Low Mass** → Minimizes scattering and energy loss :
  - Entire Detector Solenoid held under vacuum ( $\sim 10^{-4}$  torr).
  - Ultra low mass tracker.
2. **Annular** → Excludes low momentum electrons via hollow centre:
  - Inner 38 cm un-instrumented .
  - Reduces need to reject  $\sim 10^{18}$  to  $\sim 10^5$ .
  - Blind to > 99% of DIO spectrum .
3. **Segmented** → Handle high rates and provide high-precision momentum measurements.





# Minimizing Pion Backgrounds

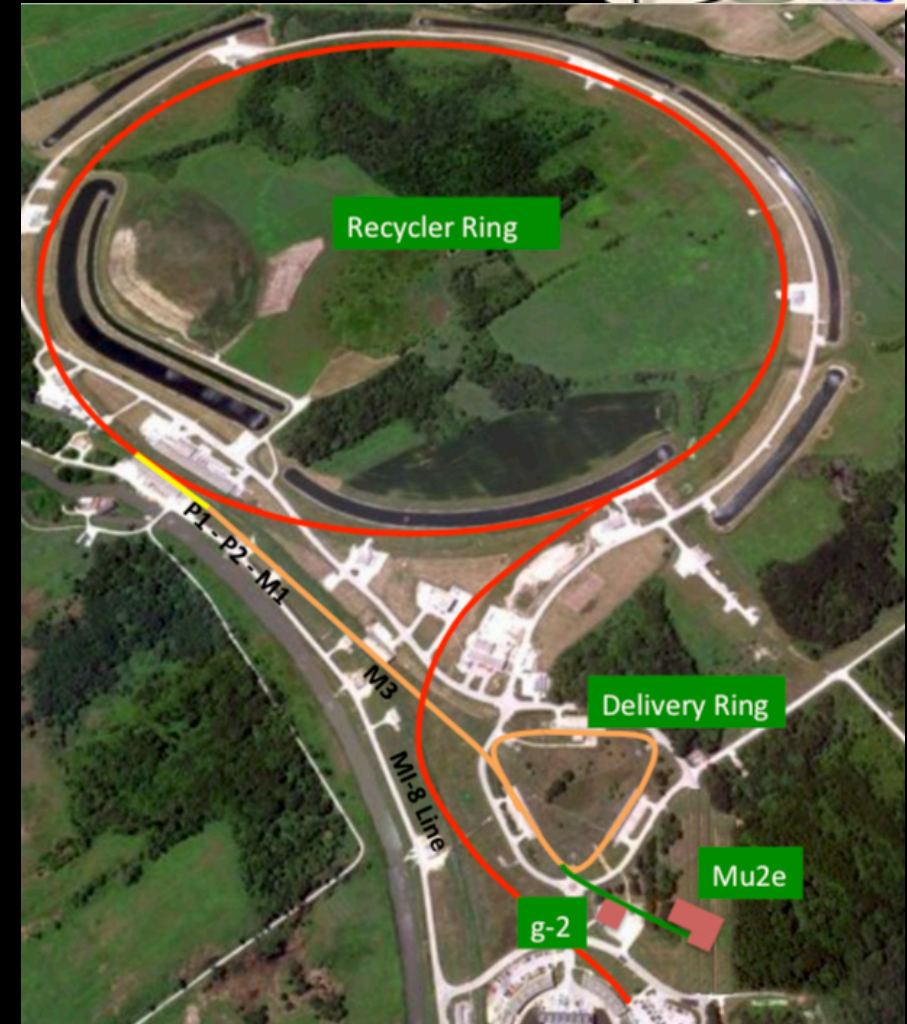
- Pions – have a free lifetime of 26ns. They decay to produce muons (and neutrinos). Muons can further decay and produce backgrounds.
- Eliminate prompt backgrounds using a primary beam of short proton pulse. Use a delayed measurement window ( $\sim 700$  ns after proton pulse at target). Before this point we ignore any tracks we see in our detector systems.



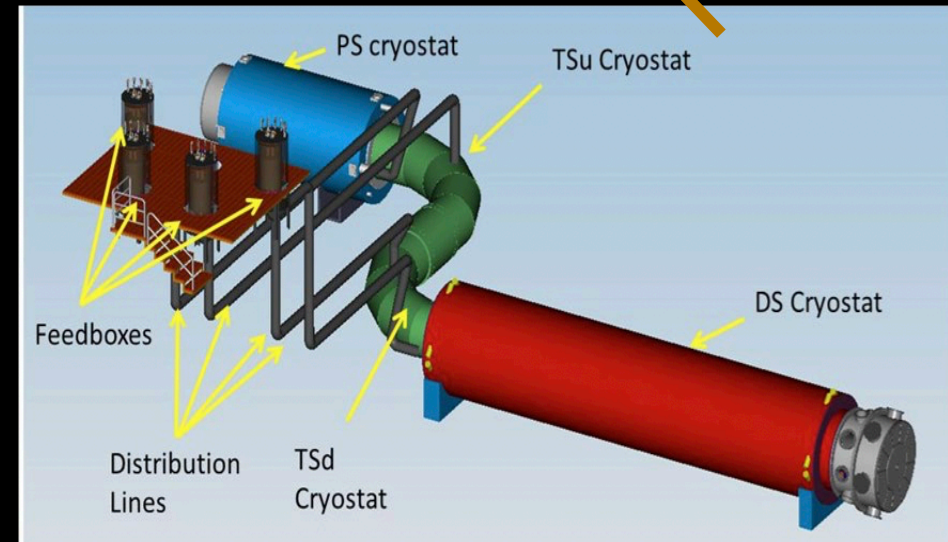
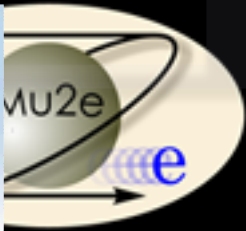
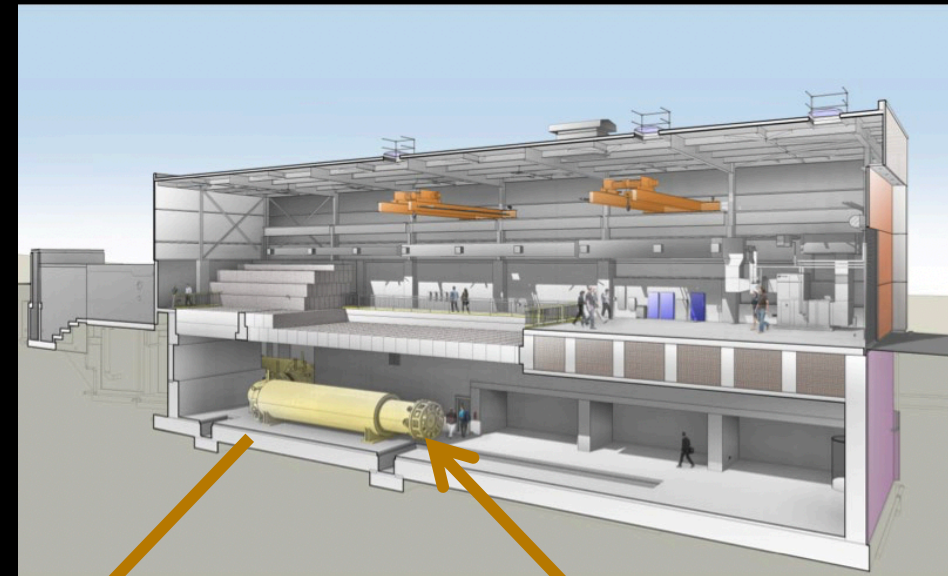
# Where do the muons come from?



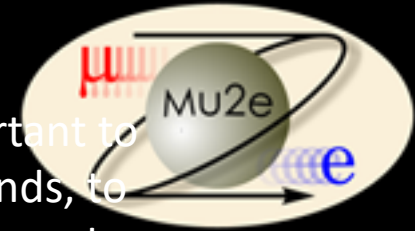
- Mu2e uses 8kW of 8 GeV protons from the Booster.
- 2 batches of  $4 \times 10^{12}$  Protons, transported from Booster via M1-8 beamline to the Recycler Ring.
- Circulate and re-bunched by a 2.5 MHz RF system.
- Reformatted bunches are kicked into the P1 line and transported to the Delivery Ring.
- They are slow extracted to the Mu2e detector through a new external beamline.
- Mu2e requires  $3.6 \times 10^{20}$  Protons on Target to reach  $3 \times 10^{-17}$  limit.



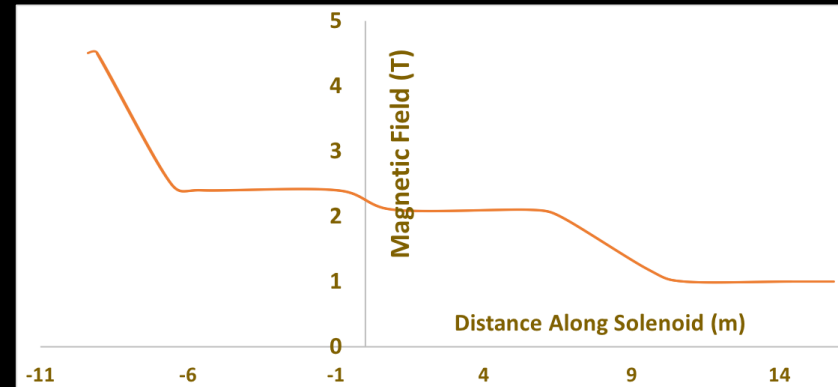




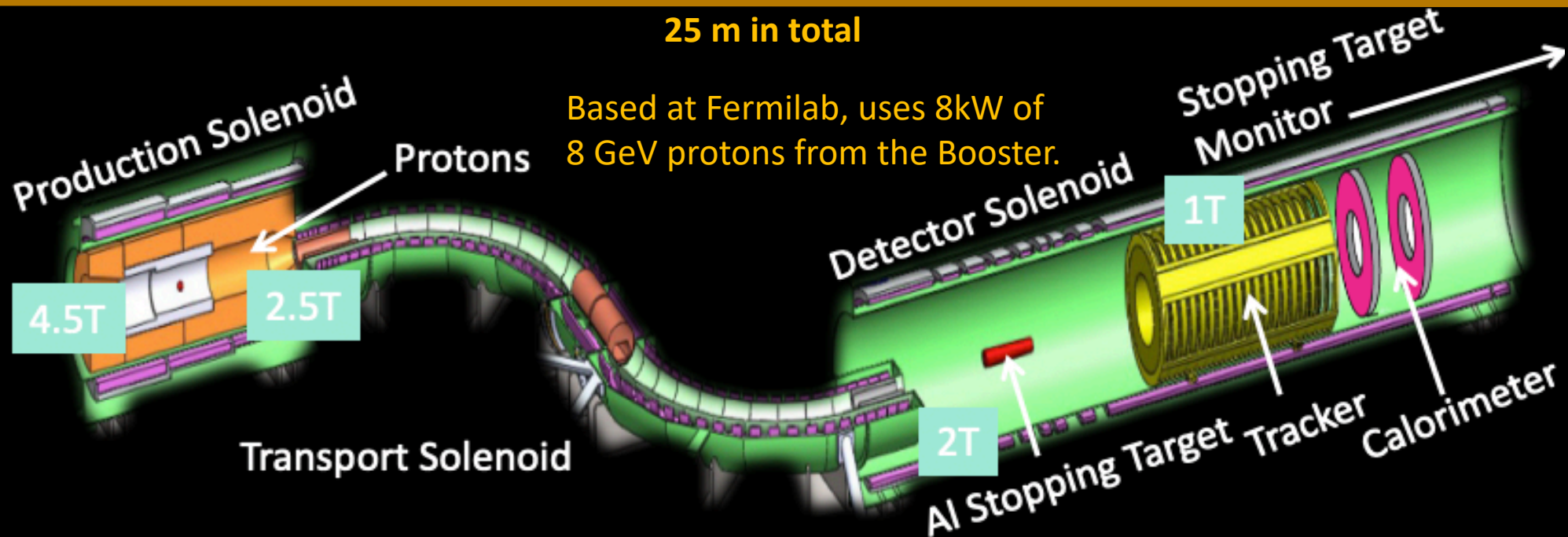
# The Mu2e Experiment



Graded fields important to suppress backgrounds, to increase muon yield, and to improve geometric acceptance for signal electrons.

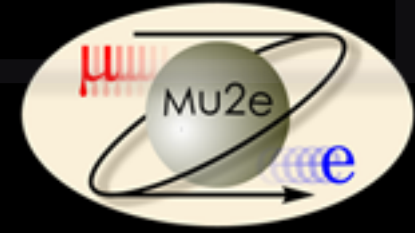


25 m in total

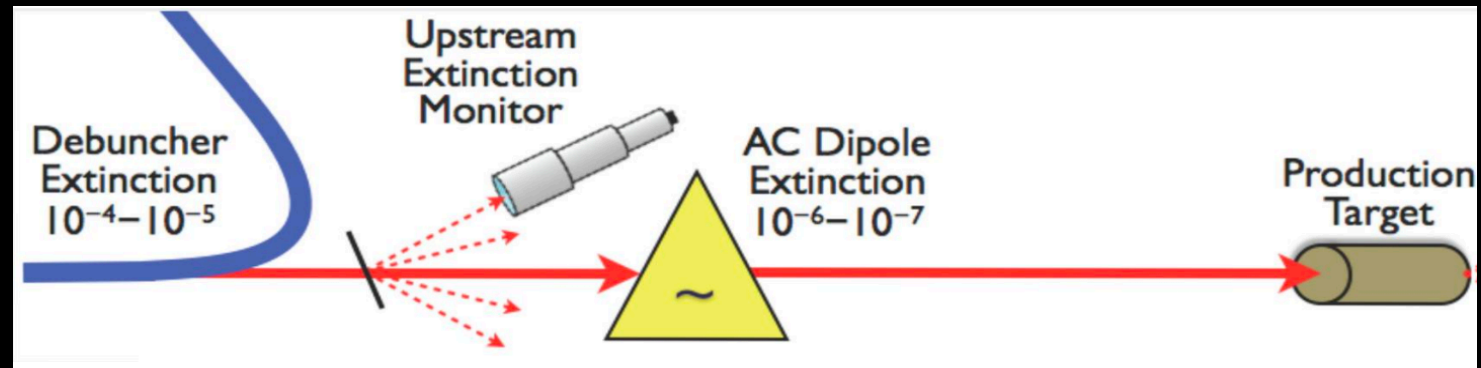




# Extinction System



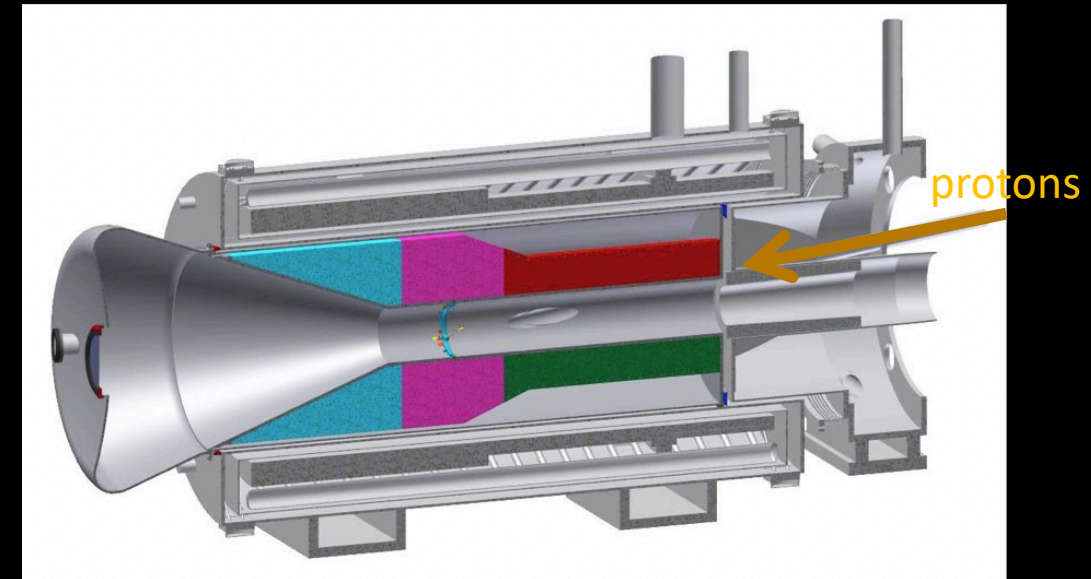
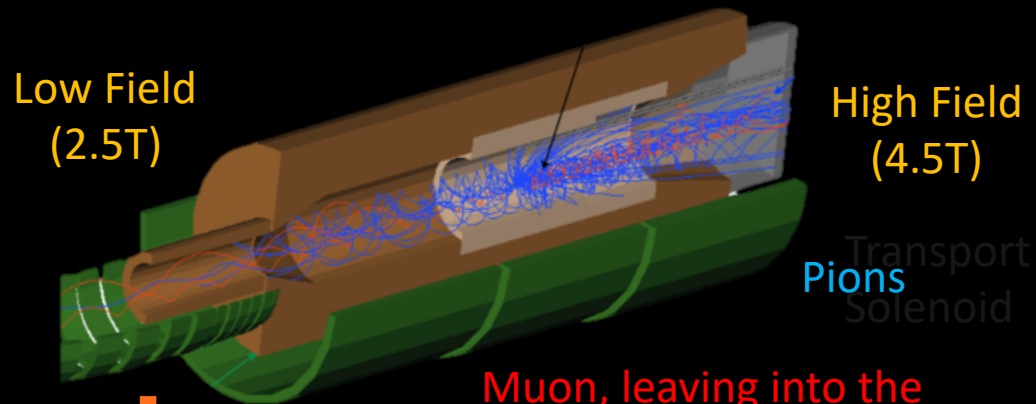
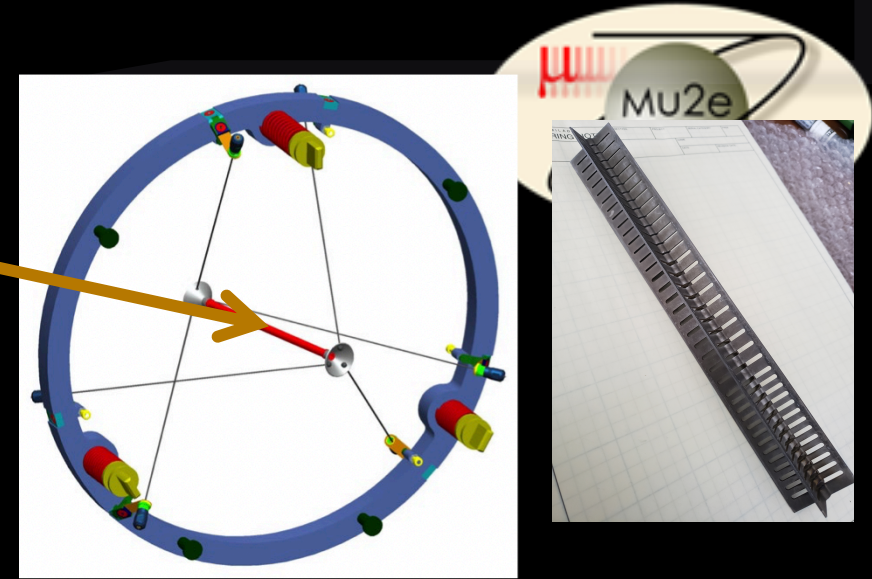
- Must have out-of-time : in-time proton ratio must be kept  $< 10^{-10}$  to remove potential backgrounds.
- 2 phase process:
  - The technique for generating the required bunch structure in the Recycler Ring leads to a high level of extinction. Fast “kicker” which transfers the proton beam from the Recycler to the Delivery Ring preserves extinction. Extinction of  $10^{-5}$  is expected as the proton beam is extracted and delivered.
  - The beam line from the Delivery Ring to the production target has a set of AC oscillating dipoles that sweep out-of-time protons into a system of collimators. This should achieve an additional extinction of  $10^{-7}$  or better.





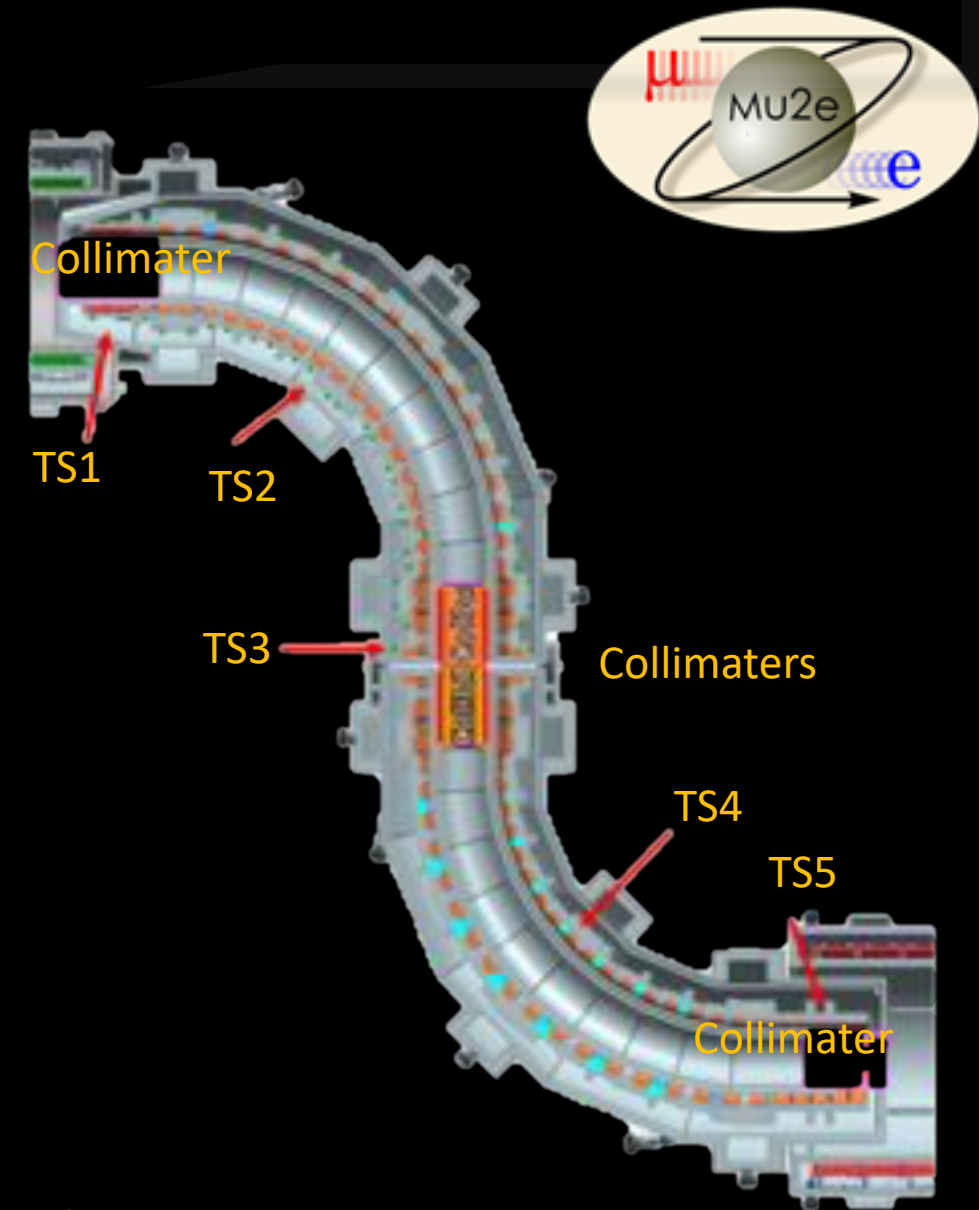
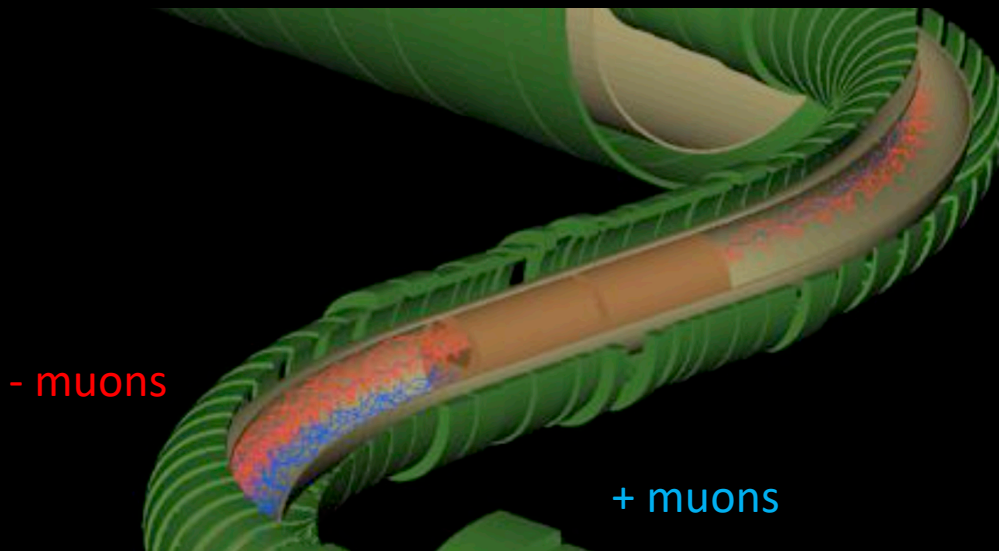
# Production Solenoid (PS)

- Protons from 8kW, 8 GeV enter and interact with Tungsten rod target.
- Target chosen to maximize pion production and minimize reabsorption.
- Pions produced, the graded magnetic field reflects the pions toward the transport solenoid.
- Target must be radiatively cooled.
- Surrounded by Heat & Radiation Shield made from Bronze. The average heat load in this shield is 3.3kW.



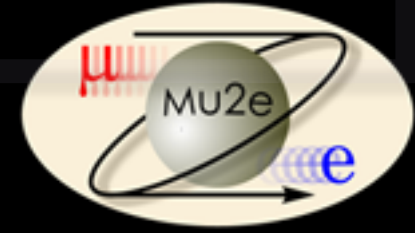
# Transport Solenoid (TS)

- Designed to optimize the transport of negative, low momentum muons from the production target to the stopping target.
- Curved solenoid eliminates line-of-sight transport of photons and neutrons .
- Curvature drift and collimators sign and momentum select beam.

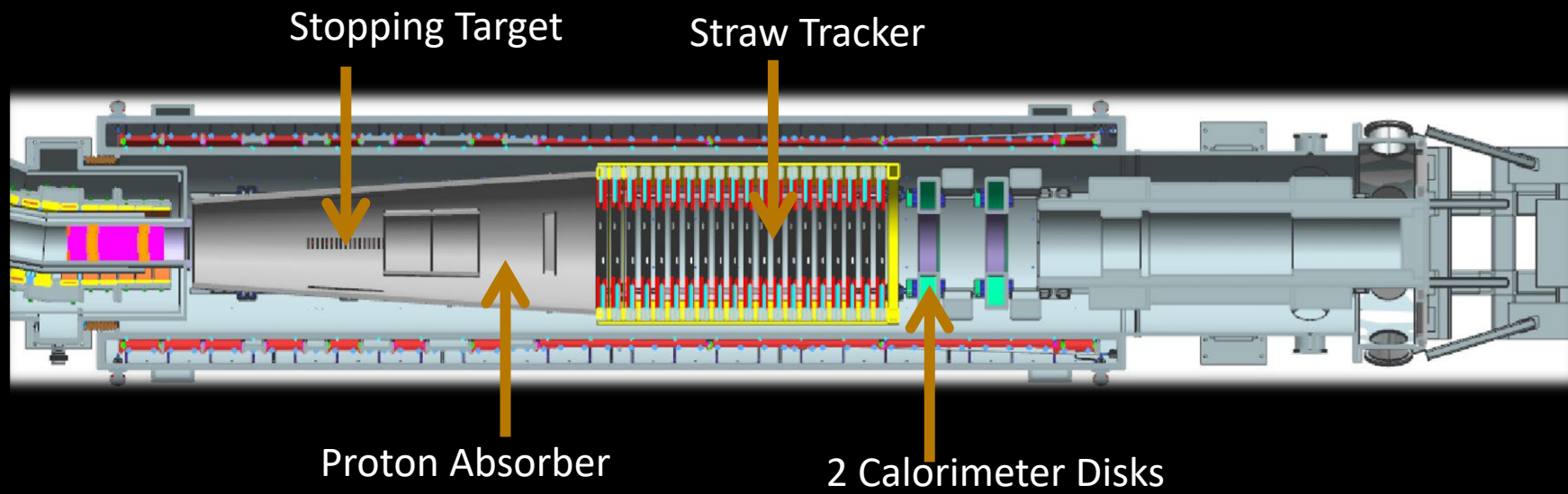


Total length of the Transport Solenoid ~13 m

# Detector Solenoid (DS)

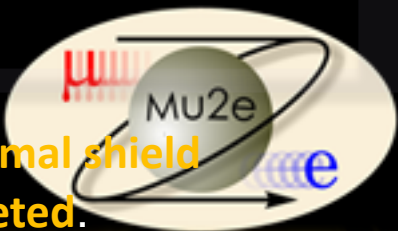


- Houses Stopping Target (ST), Straw Tracker and Calorimeter disks.
  - ~11 m long, with a clear bore diameter of ~2 m.
  - ST resides in a graded field which varies from 2T to 1 T
    - Captures conversion electrons emitted in direction opposite to detector and reflects them back.
    - Steadily increases pitch of background particles as they are accelerated towards the downstream detectors.
- The resulting pitch angle becomes inconsistent with the pitch of a conversion electron from the ST and they can be rejected.

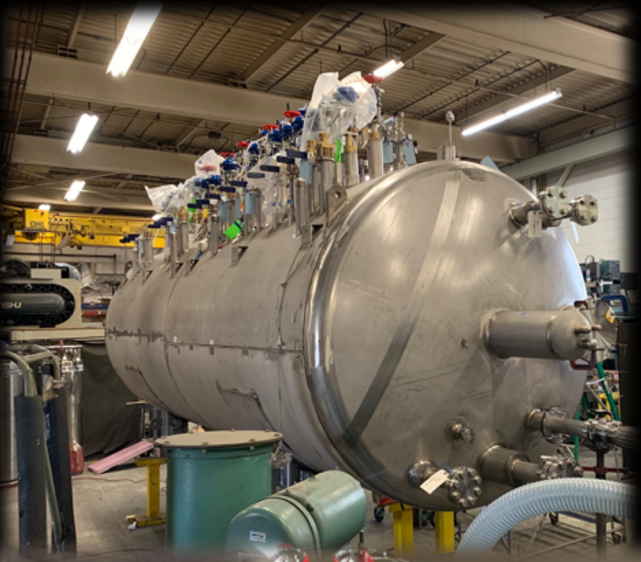




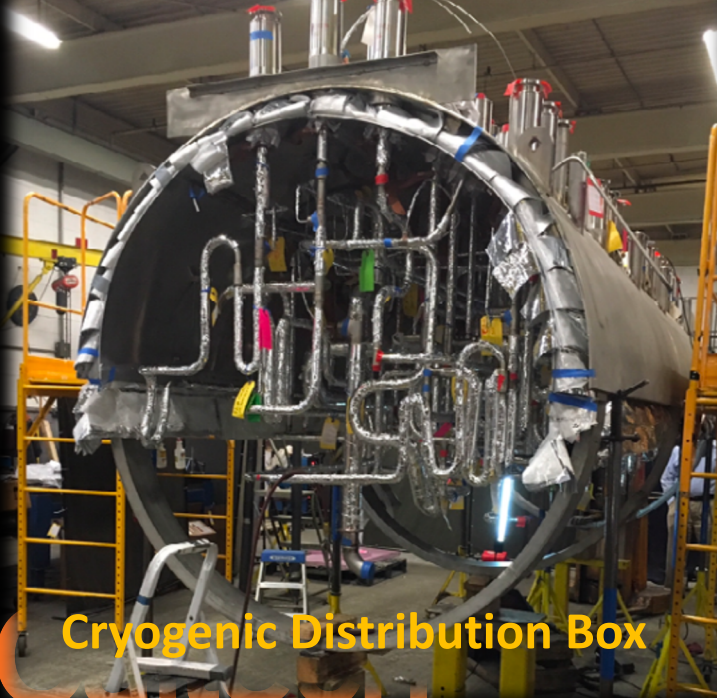
# Recent Solenoid Progress



Warm bore and thermal shield procurement completed.



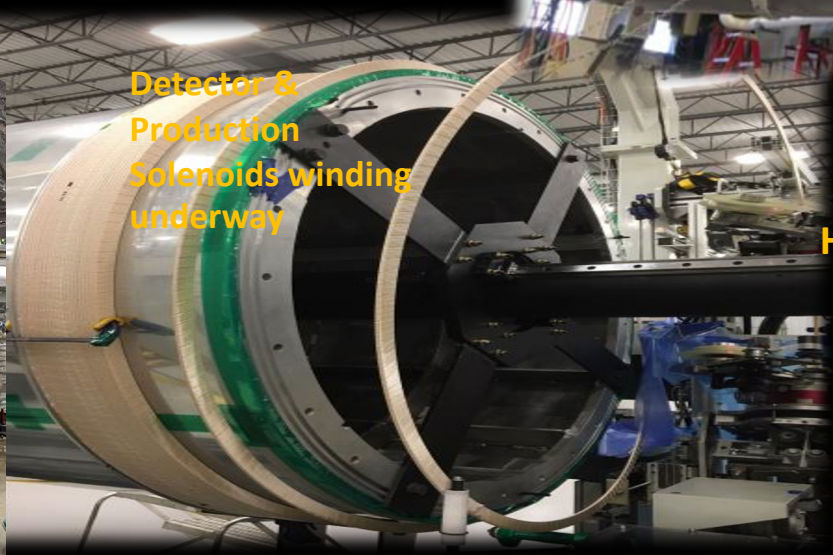
Transport Solenoid at Fermilab awaiting final tests.



Cryogenic Distribution Box



TS testing



Detector & Production Solenoids winding underway

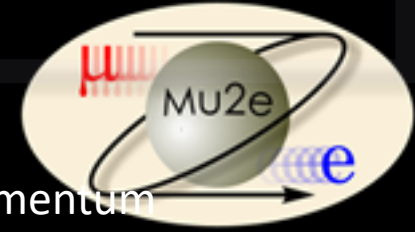
HRS construction.



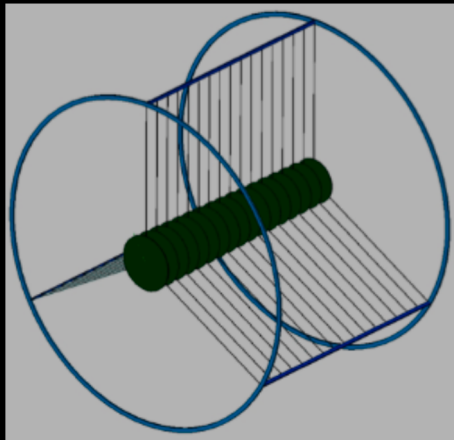
5 January 2021



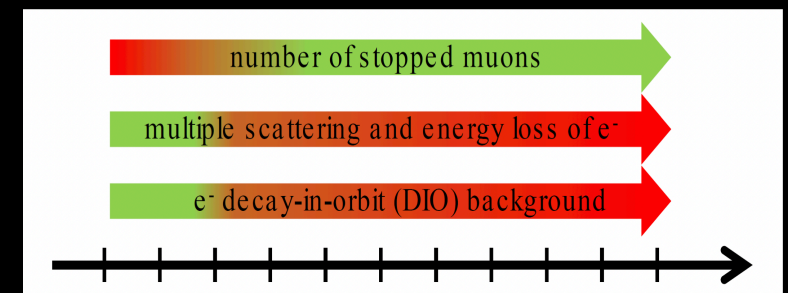
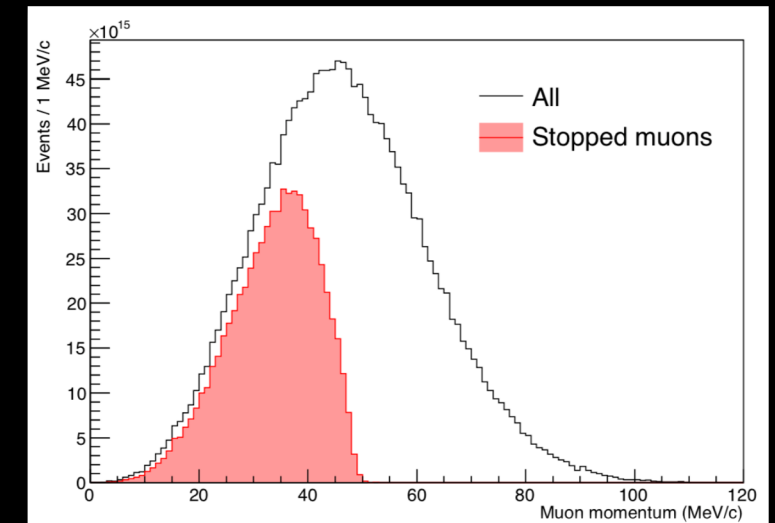
# Stopping Target (ST)



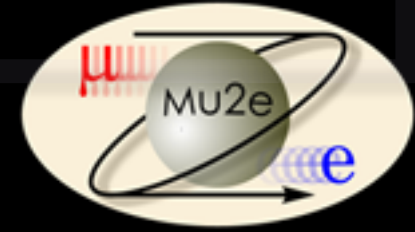
- The ST must be massive, to stop a significant fraction of incident muons, but must not corrupt the momentum measurement of conversion electrons.
- Energy loss and straggling in the stopping target are significant contributors to the momentum resolution function
- Combination of lower energy muons and a thin foil Al target help alleviate corruption.
- The number of muons stopped depends on:
  - Proton beam energy,
  - Magnetic field PS and TS,
  - The design of the collimators,
  - The ST material and geometry.
- The current design for the stopping target uses 37 thin foils.



Many effects to consider when optimizing target design:



# The Tracker: Design

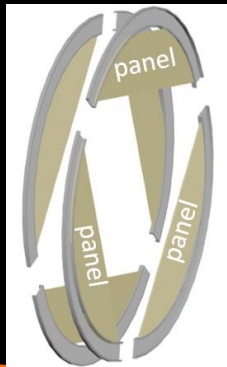


- Tracker is constructed from self-supporting panels of low mass straws tubes detectors
- 18 stations, 2 planes per station, 6 panels per plane, 96 straws per panel.
- Straw drift tubes aligned transverse to the axis of the Detector Solenoid.
  - 1m, 5 mm diameter straw
  - Walls: 12 mm Mylar + 3 mm epoxy
  - 25 mm Au-plated W sense wire
  - 33 – 117 cm in length
  - 80:20 Ar:CO<sub>2</sub> with HV < 1500 V
  - Straw wall thickness of 15 μm has never been done before
- Charged particles ionize gas – drift to wire – detect signals!

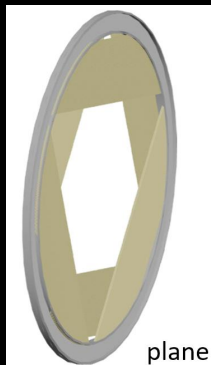
**The Straws:**



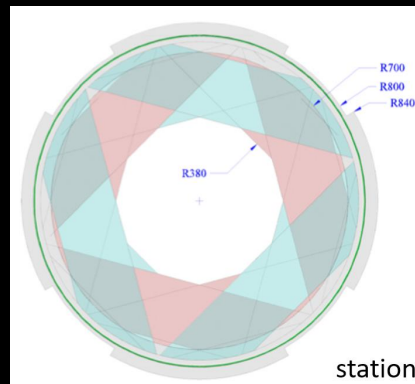
**Panels**



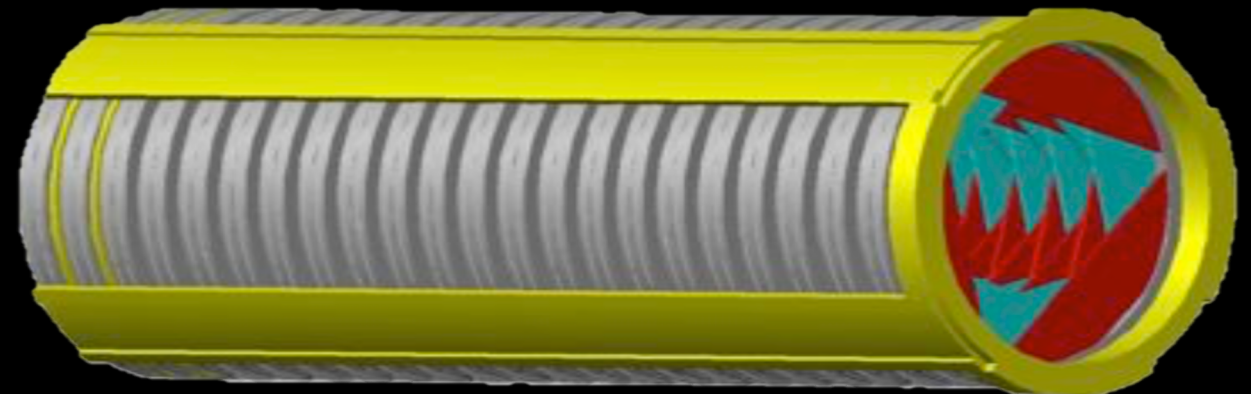
**Plane**



**Station**



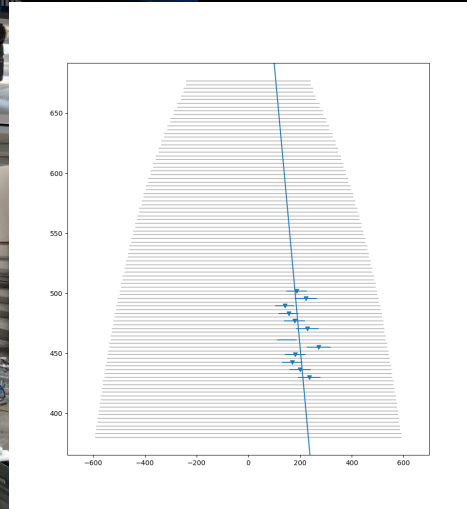
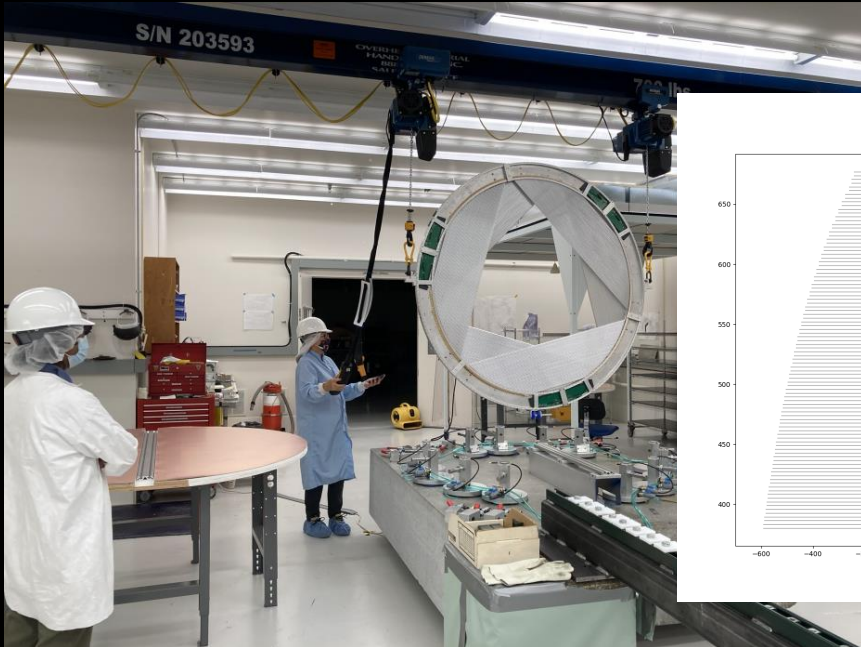
**The Tracker:** ~ 3m, 1 T field





# The Tracker: Progress

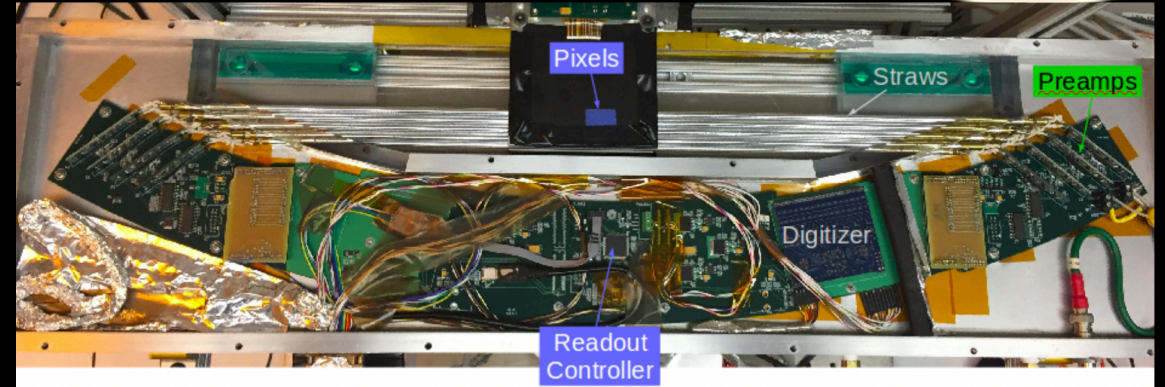
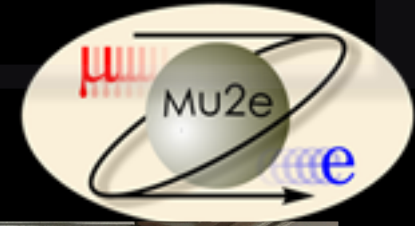
2020:



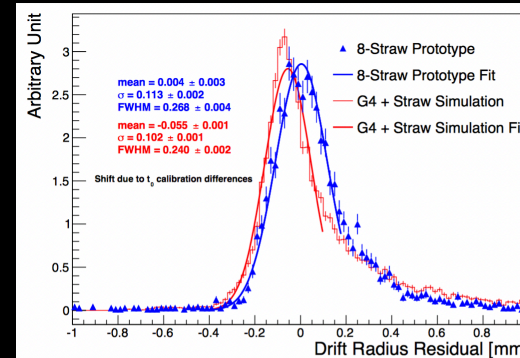
- Use Cosmic Rays.
- Use information gained to update MC.
- Measured performance and resolutions.
- Performance met requirements!

2018:

8 channel prototype



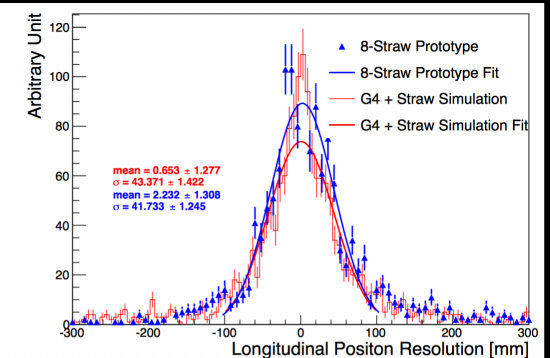
Measured gain, crosstalk, resolution...



Transverse Resolution  
(Data vs MC)

$$\sigma_{data} = 0.113 \pm 0.002 \text{ mm}$$

$$\sigma_{MC} = 0.102 \pm 0.001 \text{ mm}$$

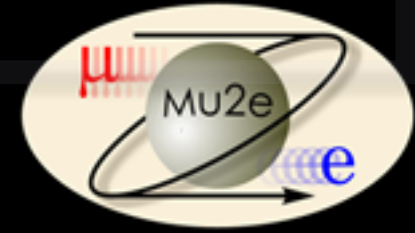


Longitudinal Resolution  
(Data vs MC)

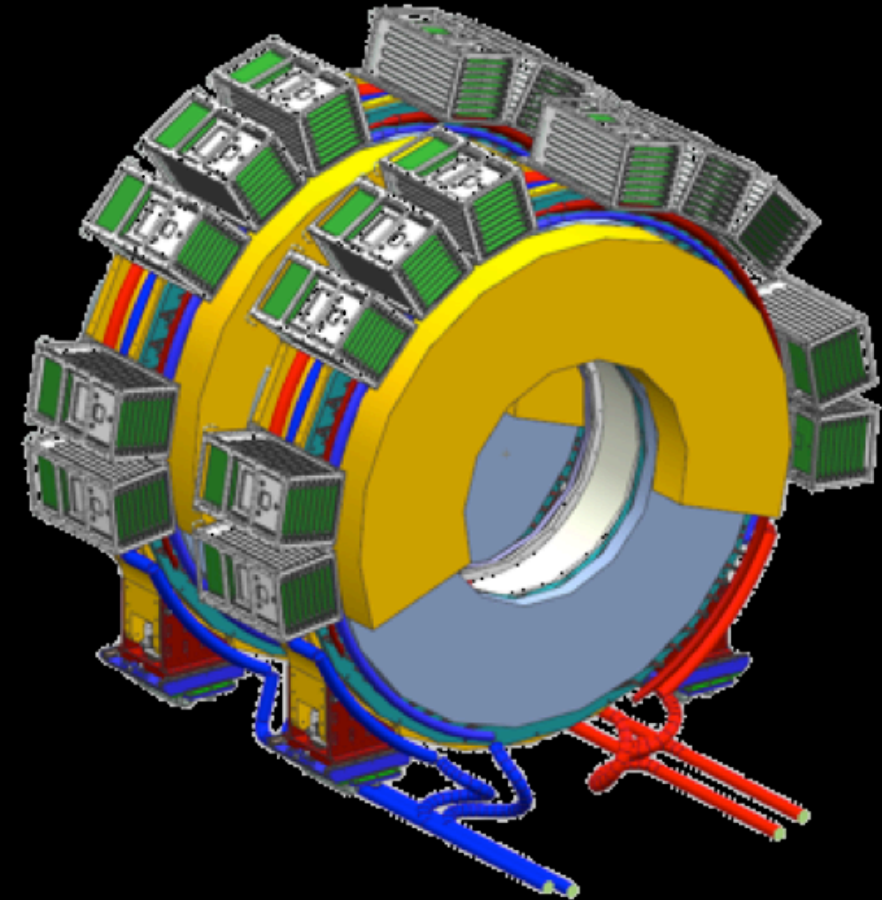
$$\sigma_{data} = 42 \pm 1 \text{ mm}$$

$$\sigma_{MC} = 43 \pm 1 \text{ mm}$$

# The Calorimeter: Purpose



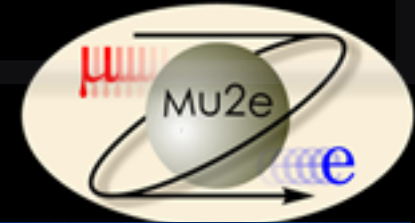
- The calorimeter is vital for providing:
  - Particle identification,
  - Fast online trigger filter,
  - Accurate timing information for background rejection
  - Seed for track reconstruction.
- The Mu2e Calorimeter must:
  - Have a large acceptance;
  - Provide time resolution  $< 0.5$  ns;
  - Energy resolution  $< 10\%$ ;
  - Position resolution of 1 cm.;
  - Function in region with radiation exposure up to 20Gy/crystal/year and with neutron flux  $10^{11}$  /cm<sup>2</sup>.
- Annular shape and 2 disks – the separation of disks is  $\frac{1}{2}$  the pitch of the mu2e signal helix, means that we cannot miss a conversion electron.



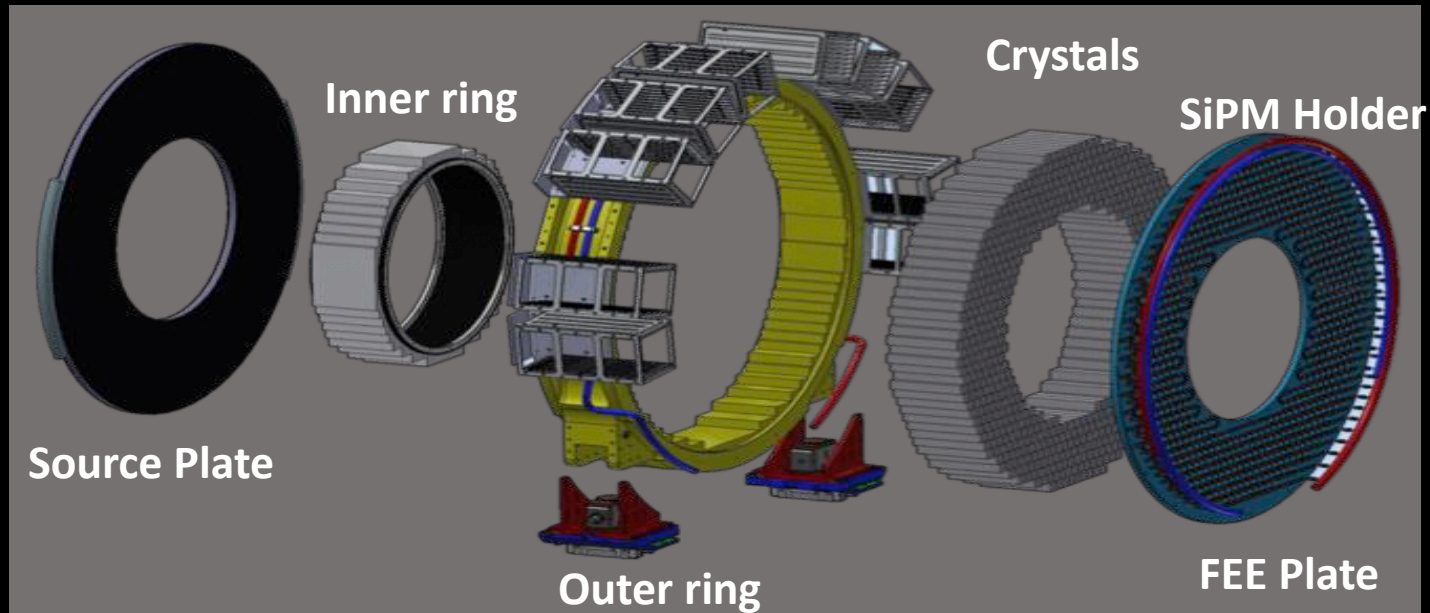


# The Calorimeter: Design

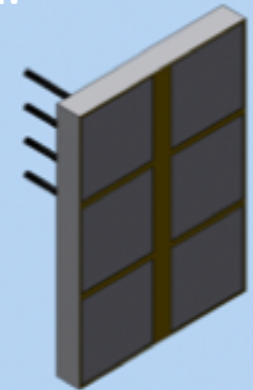
- Mu2e calorimeter uses 2 annular disks with radius 37 -66 cm.
- 674 undoped CsI (34 x 34 x 200) mm<sup>3</sup> square crystals in each disk.
- Separated by 70 cm - distance chosen so if signal electron goes down through centre it hits the next disk.
- Redundant readout - Each crystal 2 UV-extended SiPMs.
- 1 FEE/SiPM - SiPM holders with front end electronics (FEE) are inserted into the backplane.



## Crystals:

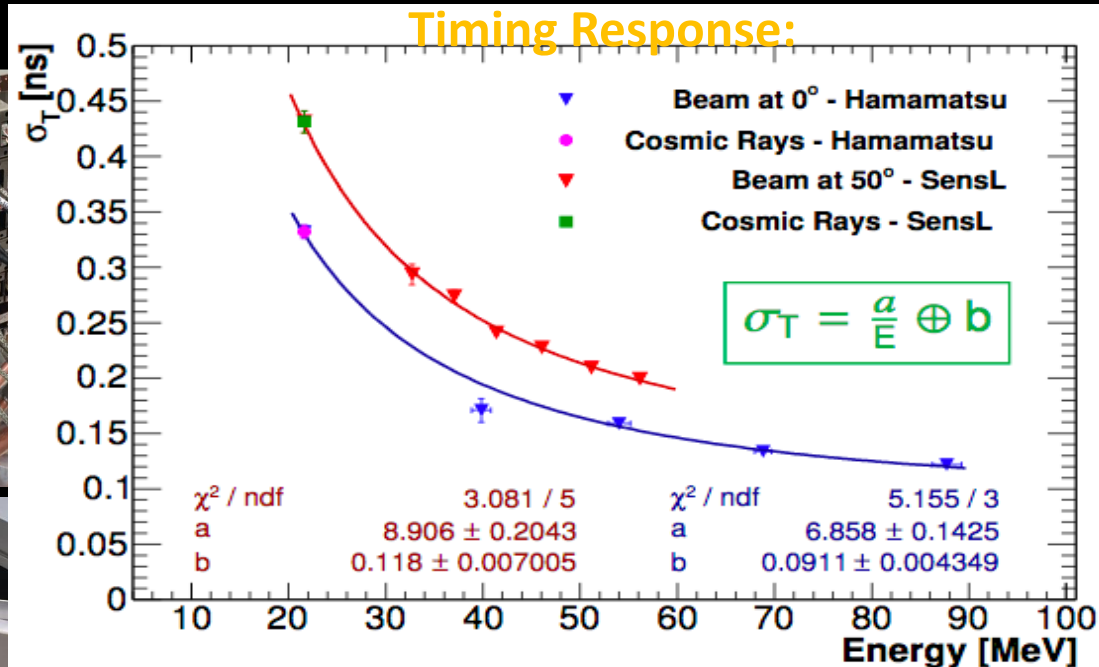


## SiPM:

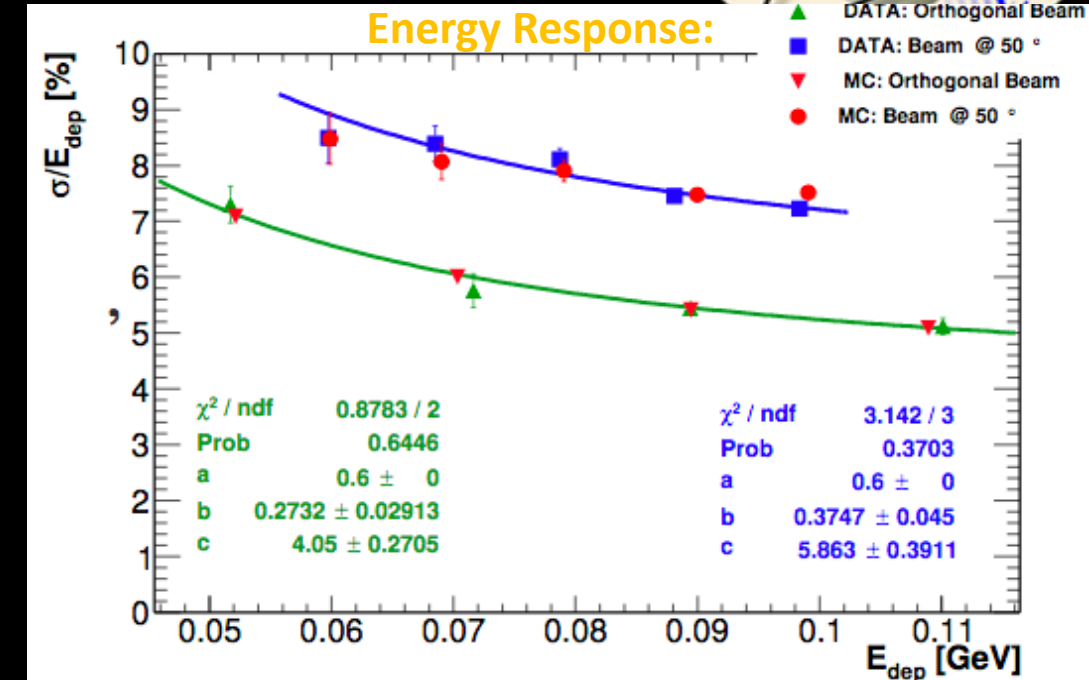


# The Calorimeter: Progress

- R&D and Prototyping successfully completed.
- All Crystals and SiPMs procured and now at FNAL, assembly begins imminently.



Typical time resolution  
 $E_{\text{beam}} @ 100 \text{ MeV}$   
 $\sigma_{T1} \sim 130 \text{ ps}$



- Test beam with  $e^-$  with  $E = 60\text{-}120 \text{ MeV}$ .
- Good agreement between MC/Data!
- Meets energy and timing performance requirements!

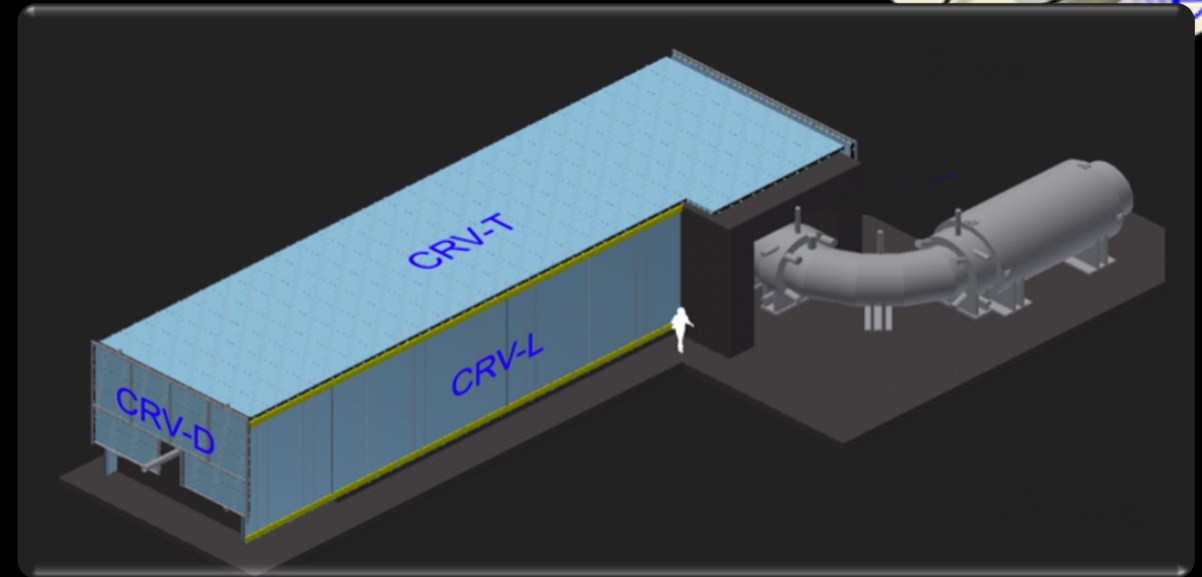
# The Cosmic Ray Veto

Each day,  $\sim 1$  conversion-like electron is produced by cosmic rays

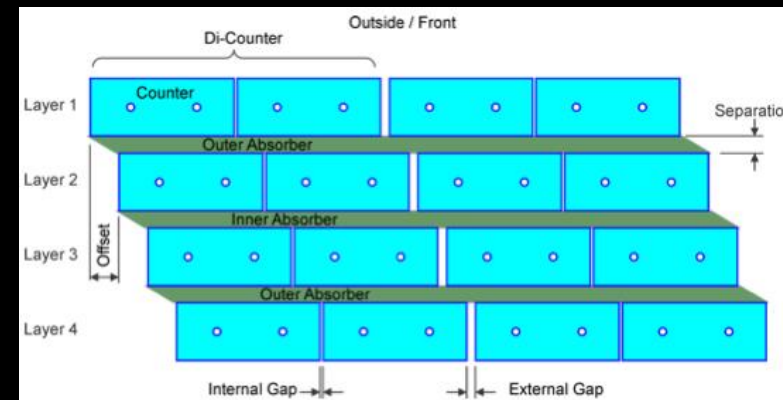


Cosmic Ray Veto will prevent cosmic muons faking a signal:

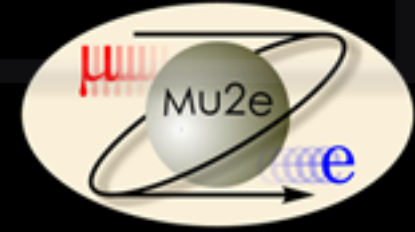
- 4 layers of extruded polystyrene scintillator counter.
- Surrounds the top and sides of DS and the downstream end of the Transport Solenoid.
- Suppresses the spurious detection of conversion-like particles initiated by cosmic-ray muons.
- 99.99% efficiency requirement!



Each panel is composed of  $5 \times 2 \times 450 \text{ cm}^3$  scintillator bars:

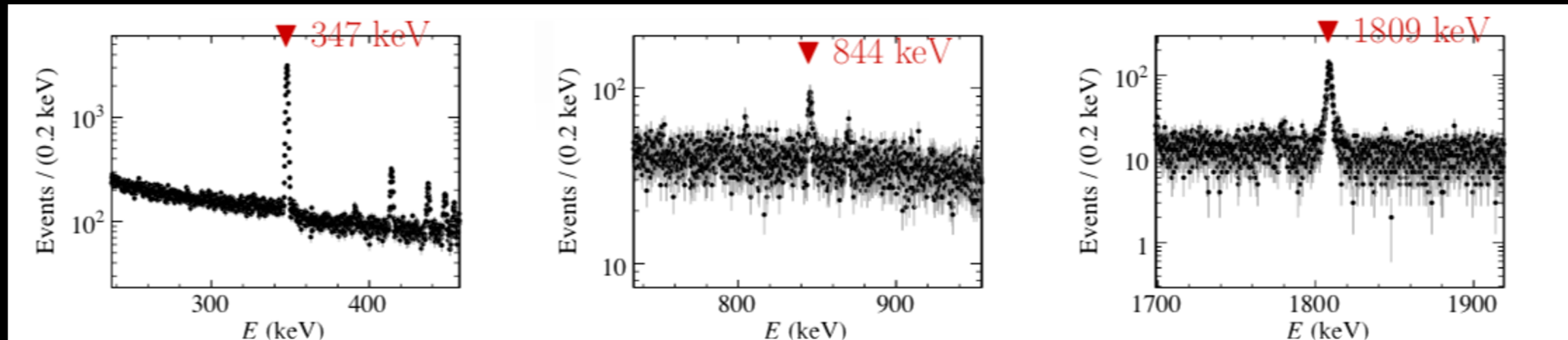


# The Stopping Target Monitor (STM)



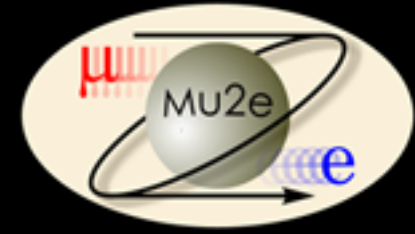
- Need an accurate measure of total number of stopped muons in the target (within 10%).
- Placed far downstream of Detector Solenoids (~34 m from target).
- STM uses HPGe and LaBr<sub>3</sub> detectors to measure X/gamma-rays produced by stopped muons in Al target:
  - Prompt X-ray emitted from muonic atoms at 347keV;
  - Delayed gamma ray at 844keV;
  - Semi-prompt gamma ray at 1.809MeV.

$$R_{\mu e} = \frac{\Gamma(\mu^- + A(Z, N) \rightarrow e^- + A(Z, N))}{\Gamma(\text{all} - \text{captures})} < 7 \times 10^{-13} (90\% \text{C.L.})$$





# Mu2e: Current Status



- Mu2e construction is nearly complete:
  - Beamline is finished.
  - Superconducting cable for all solenoids procured, winding for all three solenoid units is well-underway.
  - Transport Solenoid coils arrived at Fermilab, final testing and assembly underway.
  - Tracker straws, FEE prototypes, calorimeter crystals and SiPMs, STM detectors, and CRV counters are complete.
  - Assembly and testing of these detector components is on-going.
- Transition to installation in 2021;
- Detector commissioning beginning in 2022;
- Commissioning with beam continuing through 2023;
- Physics running is expected to begin in 2024.

2020: Transport Solenoid at FNAL





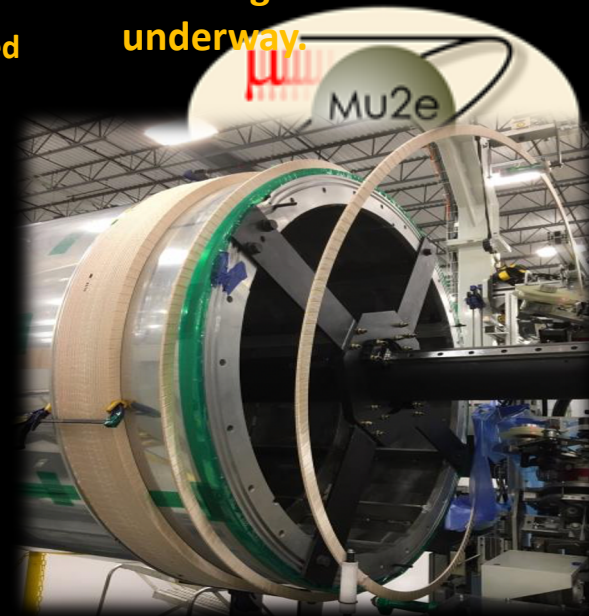
# Mu2e: Status



**Mu2e Building complete**

**2020: All Calorimeter Crystals delivered and tested. Assembly beginning.**

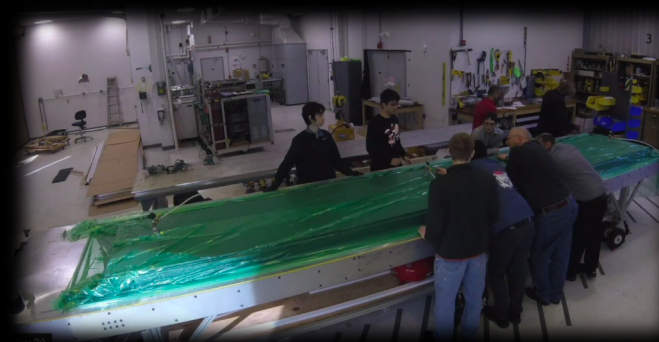
**Winding of DS and PS well underway.**



**2020: Transport Solenoid assembled and tested at FNAL**



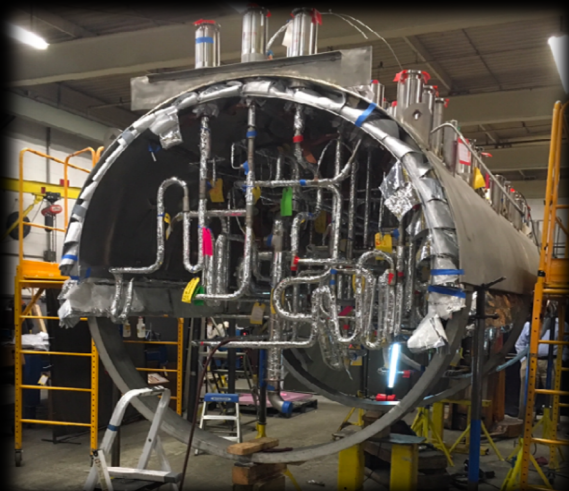
**Cosmic Ray Veto Assembly on going**



**Straw Tracker construction ongoing**



**2019: Warm bore and thermal shield procurement completed.**

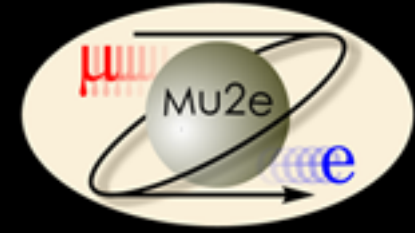


**2019: Cryogenic Distribution Box constructed**

**2019: Completed transfer lines**



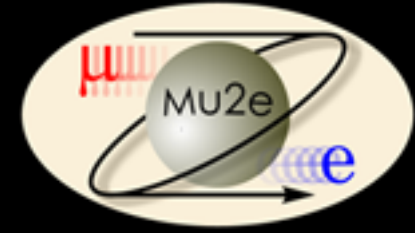
# Summary



- Muon CLFV channels offer deep indirect probes into BSM.
- Mu2e is at the forefront of active global CLFV program. Discovery potential over a wide range of well motivated BSM models.
- Muon-to-electron sector complements tau and Higgs collider searches such as:  $\tau \rightarrow e\gamma$  or  $\mu\gamma$  and  $H \rightarrow e\tau, \mu\tau$ , or  $\mu e$ .
- It is important to eliminate Standard Model backgrounds so the experiment is designed to be “background free”:
  - Super conducting solenoids to collect and efficiently transport low momentum muons;
  - Pulsed beam removes backgrounds from pions;
  - Low mass, annular tracker has high resolution to avoid DIO backgrounds;
  - Cosmic Ray Veto surrounds detectors to remove “fake signals” from Cosmic muons.

*Thank You for listening!*

# Complementary Searches



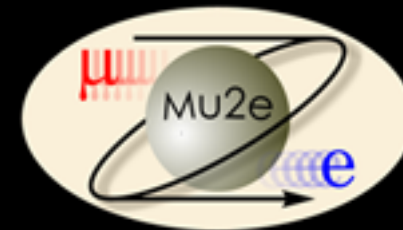
$$\mu^- N \rightarrow e^+ N$$

- This conversion violates both lepton number ( $\Delta L = 2$ ) and lepton flavor conservation, and can only proceed if neutrinos are Majorana particles.
- The Mu2e sensitivity to  $\mu^- \rightarrow e^+$  extends beyond the current best limit: [Phys Rev Lett B 412 p 334-338 \[13\]](#)
- $\langle m_{e\mu} \rangle$  effective Majorana neutrino mass scale sensitivity down to the MeV region, surpassing the  $\langle m_{\mu\mu} \rangle$  sensitivity in the kaon sector which is limited to the GeV region

$$\mu^- N \rightarrow e X N$$

- Where X is a new light boson (or axion).
- Feasibility under study.
- On example parameterization: [arXiv: 1110.2874](#)





# Useful Resources

1. S. T. Petcov, Sov. J. Nucl. Phys. **25**, 340 (1977); Yad. Fiz. **25**, 1336 (1977) [erratum].
2. S. M. Bilenky, S. T. Petcov, and B. Pontecorvo, Phys. Lett. B **67**, 309 (1977).
3. W. J. Marciano and A. I. Sanda, Phys. Lett. B **67**, 303 (1977).
4. B. W. Lee, S. Pakvasa, R. E. Shrock, and H. Sugawara, Phys. Rev. Lett. **38**, 937 (1977); **38**, 1230 (1977) [erratum].
5. J. Adam *et al.* (EG Collaboration), Phys. Rev. Lett. **110**, 20 (2013).
6. W. Bertl *et al.* (SINDRUM-II Collaboration), Eur. Phys. J. **C47**, 337 (2006).
7. U. Bellgardt *et al.*, (SINDRUM Collaboration), Nucl. Phys. **B299**, 1 (1988).
8. A.M. Baldini *et al.*, “MEG Upgrade Proposal”, arXiv:1301.7225v2 [physics.ins- det].
9. Y. Kuno *et al.*, “COMET Proposal” (2007)
10. Mu2e TDR, arXiv:1501.05241
11. Nuclear Physics B - Proceedings Supplements Volumes 248–250, March–May 2014, Pages 35-4
12. A. Czarnecki *et al.*, “Muon decay in orbit: Spectrum of high-energy electrons,” Phys. Rev. D **84** (Jul, 2011) .
13. Sindrum-II “Improved limit of Branching Fraction of  $\mu^- \rightarrow e^+$  in Titanium”, Phys Lett B **422** (1998) 334-338 (1998)